# Update a biogeochemical model with process-based algorithms to predict ammonia volatilization from fertilized cultivated uplands and rice paddy fields

Siqi Li[1], Wei Zhang[1], Xunhua Zheng[1, 2], Yong Li[1], Shenghui Han[1], Rui Wang[1], Kai Wang[1], Zhisheng Yao[1], Chunyan Liu[1], Chong Zhang[3]

[1]State Key Laboratory of Atmospheric Boundary Layer Physics and Atmospheric Chemistry, Institute of Atmospheric Physics, Chinese Academy of Sciences, Beijing 100029, P. R. China

[2]College of Earth and Planetary Science, University of Chinese Academy of Sciences, Beijing 100049, P.R. China

[3]College of Tropical Crops, Hainan University, Haikou 570228, China

*Correspondence to*: Xunhua Zheng (xunhua.zheng@post.iap.ac.cn)

Yong Li (yli@mail.iap.ac.cn)

**Abstract.** Accurate simulation of ammonia ($NH_3$) volatilization from fertilized croplands is crucial to enhancing fertilizer-use efficiency and alleviating environmental pollution. In this study, a process-oriented model, CNMM-DNDC (Catchment Nutrient Management Model - DeNitrification-DeComposition), was evaluated and modified using $NH_3$ volatilization observations from 44 and 19 fertilizer application events in cultivated uplands and paddy rice fields in China, respectively. The major modifications for simulating $NH_3$ volatilization from cultivated uplands were primarily derived from a peer-reviewed and published study. $NH_3$ volatilization from cultivated uplands was jointly regulated by wind speed, soil depth, clay fraction, soil temperature, soil moisture, vegetation canopy, and rainfall-induced canopy wetting. Moreover, three principle modifications were made to simulate $NH_3$ volatilization from paddy rice fields. First, the simulation of the floodwater layer and its pH were added. Second, the effect of algal growth on the diurnal fluctuation of floodwater pH was introduced. Finally, the Jayaweera-Mikkelsen model was introduced to simulate $NH_3$ volatilization. The results indicated that the original CNMM-DNDC not only performed poorly in simulating $NH_3$ volatilization from cultivated uplands but also failed to simulate $NH_3$ volatilization from paddy rice fields. The modified model showed remarkable performances in simulating the cumulative $NH_3$ volatilization of the calibrated and validated cases, with drastically significant zero-intercept linear regression of slopes of 0.94 ($R^2$ = 0.76, $n$ = 40) and 0.98 ($R^2$ = 0.71, $n$ = 23), respectively. The

simulated $NH_3$ volatilization from cultivated uplands was primarily regulated by the dose and type of the nitrogen fertilizer and the irrigation implementation, while the simulated $NH_3$ volatilization from rice paddy fields was sensitive to soil pH, the dose and depth of nitrogen fertilizer application, and flooding management strategies, such as floodwater pH and depth. The modified model is acceptable to compile regional or national $NH_3$ emission inventories and developing strategies to alleviate environmental pollutions.

**1. Introduction**

Synthetic fertilizer application, as the secondary largest contributor to ammonia ($NH_3$) emissions after livestock production, accounts for approximately 30% to 50% of anthropogenic $NH_3$ emissions (Behera et al., 2013; Bouwman et al., 1997; Huang et al., 2012; Paulot et al., 2014). The great quantity of $NH_3$ volatilized from agricultural fields contributes to low nitrogen use efficiency for crops (Chien et al., 2009; Mariano et al., 2019; Zhu et al., 1989). The subsequent dry and wet deposition to terrestrial ecosystems results in the acidification and eutrophication of natural ecosystems (e.g., Anderson et al., 2008; Bobbink et al., 1998; Li et al., 2016) and is also considered an indirect source of nitrous oxide (Martin et al., 2004; Schjørring, 1998). Recently, $NH_3$ in the atmosphere has played a vital role in aerosol formation during several haze periods, which has attracted great attention (e.g., Felix et al., 2013; Kong et al., 2019; Liu et al., 2018; Savard et al., 2017).

Many studies have attempted to estimate $NH_3$ loss from fertilized croplands using biogeochemical process models, i.e., DeNitrification-DeComposition (DNDC), and water and nitrogen management (WNMM) and CESM (Dubache et al., 2019; Dutta et al., 2016; Giltrap et al., 2017; Michalczyk et al., 2016; Park et al., 2008; Riddick et al., 2016; Vira et al., 2020). However, these models do not distinguish between the simulation modules of $NH_3$ volatilization for cultivated uplands and rice paddy fields but rather use the same algorithm (Cannavo et al., 2008; Li, 2016). It is worth emphasizing that the mechanisms of $NH_3$ volatilization are completely different between cultivated uplands and rice paddy fields due to the presence of floodwater over rice paddy soils. Recent studies also indicate that estimating $NH_3$ emissions without considering rice cultivation results in large uncertainties (Riddick et al., 2016; Xu et al., 2019). In particular, some studies have shown that $NH_3$ volatilization rates from rice paddy fields are not lower than those of upland crops (Zhou et al., 2016), which also indicates the different mechanisms of $NH_3$ volatilization between cultivated uplands and rice paddy fields. Therefore, using separate modules to simulate $NH_3$ volatilization from cultivated uplands and rice paddy fields is necessary for the accurate estimation of $NH_3$ emissions.

Given the totally different mechanisms of $NH_3$ volatilization between cultivated uplands and rice paddy fields, the influencing factors affecting $NH_3$ volatilization from cultivated uplands are different from those of rice paddy fields. The dose, type and application methods of nitrogen fertilizer have been confirmed as the primary factors affecting $NH_3$ volatilization from cultivated uplands (e.g., Liu et al., 2003; Roelcke et al., 2002; Zhang et al., 1992). Moreover, several studies have reported that irrigation and precipitation exert a complicated influence (stimulated or inhibited) on $NH_3$ volatilizations from cultivated uplands (e.g., Han et al., 2014; Holcomb III et al., 2011; Sanz-Cobena et al., 2011). However, the depth and pH of surface floodwater, which are unique characteristics of rice paddy fields, were found to be the major factors influencing $NH_3$ volatilization from rice paddy fields (Bowmer and Muirhead, 1987; Hayashi et al., 2006; Jayaweera and Mikkelsen, 1991). A comprehensive discussion of the influencing factors affecting $NH_3$ volatilization from cultivated uplands and rice paddy fields is crucial for providing suggestions to further improve the performance of process-based biogeochemical models in simulating $NH_3$ volatilization from cropland soils and offer specific and pertinent policy advice for the reduction of $NH_3$ loss.

A previous study established a scientific algorithm for the DNDC model to simulate $NH_3$ volatilization from cultivated uplands, which performed well under validation with independent cases of cultivated uplands from China (Li et al., 2019). However, no biogeochemical model has achieved simulations of $NH_3$ volatilization from rice paddy fields using a process-oriented algorithm, although a classical and extensively used model, i.e., the Jayaweera-Mikkelsen model (J-M model), exists (Jayaweera and Mikkelsen, 1990a; Li et al., 2008; Wang et al., 2016; Zhan et al., 2019).

The Catchment Nutrient Management Model-DeNitrification-DeComposition (CNMM-DNDC) model, established by coupling the core carbon and nitrogen biogeochemical processes of DNDC (e.g., decomposition, nitrification, denitrification and fermentation) into the distributed hydrologic framework of CNMM, is one of the latest versions of DNDC (Zhang et al., 2018). The CNMM-DNDC has been gradually developing into a comprehensive and reliable process-oriented biogeochemical model that performs well in terms of simulating the complex hydrologic and biogeochemical processes of a subtropical catchment with various landscapes (Zhang et al., 2018), the nitrous oxide and nitric oxide emissions from a subtropical tea plantation (Zhang et al., 2020) and the $NO_3^-$ leaching processes of black soils in northeastern China (Zhang et al., 2021). However, the rationality of the CNMM-DNDC's scientific processes in simulating $NH_3$ volatilization from fertilized croplands is still lacking in terms of a thorough assessment. In particular, CNMM-DNDC and other widely used biogeochemical models (e.g., DNDC) do not consider floodwater over rice paddy soils when simulating $NH_3$ volatilization but rather directly adopt the scientific processes and algorithms applied in $NH_3$ volatilization from cultivated uplands to predict $NH_3$ volatilization from rice paddy fields (Li, 2016; Zhang et al., 2018).

Based on the above deficiencies, the authors hypothesized that the CNMM-DNDC is able to simulate $NH_3$ volatilization following the application of synthetic nitrogen fertilizers to cultivated uplands and flooded rice paddy fields. To test this hypothesis, this study evaluated and modified the CNMM-DNDC's scientific processes for simulating $NH_3$ volatilization from cropland soils using 44 and 19 fertilizer application events from cultivated uplands and rice paddy fields in China, respectively. The objectives of this study were to (i) evaluate the performance of the CNMM-DNDC in simulating the observed $NH_3$ volatilization following synthetic nitrogen application to cultivated uplands, (ii) introduce thoroughly tested and validated scientific algorithms simulating $NH_3$ volatilization from cultivated uplands into the CNMM-DNDC, (iii) adopt widely applied process-based algorithms (J-M model) into the modified CNMM-DNDC, (iv) assess the performance of the modified model to simulate $NH_3$ volatilization from flooded rice paddy fields using collected reliable observations, and (v) identify the major factors affecting $NH_3$ volatilization from cultivated uplands and rice paddy fields to offer suggestions for further improving the model performance.

## 2. Materials and methods

### 2.1 Model introduction and modifications

#### 2.1.1 Brief introduction of the CNMM-DNDC

The CNMM-DNDC model was originally established by Zhang et al. (2018). In the original CNMM-DNDC, the core biogeochemical processes (including decomposition, nitrification, denitrification and fermentation) of DNDC (Li, 2016; Li et al., 1992) were incorporated into the distributed hydrologic framework of CNMM (Li et al., 2017). Based on comprehensive observations, the CNMM-DNDC was initially tested in a subtropical catchment, which showed credible performances in simulating the yields of crops, emissions of greenhouse gases (i.e., methane and nitrous oxide), emissions of nitrogenous pollutant gases (i.e., nitric oxide and $NH_3$), and hydrological nitrogen losses by leaching and $NO_3^-$ discharge in streams for different land uses (including forests and arable lands cultivated with maize, wheat, oil rape, or rice paddy) (Zhang et al., 2018). Subsequently, Zhang et al. (2020) modified the CNMM-DNDC by adding tea growth-related processes that may induce a soil pH reduction, and this modified model performed well in simulating the emissions of nitrous oxide and nitric oxide from a subtropical tea plantation plot. Moreover, the CNMM-DNDC performed well in simulating the $NO_3^-$ leaching process of black soils in northeastern China (Zhang et al., 2021). However, during model preparation and operation for the simulation of $NH_3$ volatilization, the authors found that the present model version, using a complicated and obscure R programming script to prepare the ARC GRID ASCII data format of site/plot-scale inputs, was time-consuming and confusing. Therefore, an easy-to-operate and standardized version of the model needed to be established. Thus, a standardized model version was established in this study.

The new standard version of the model was built without changing the original key scientific modules; however, the complicated R programming script was converted into a simple Excel spreadsheet to prepare the model inputs, which is easy for beginners to use. The site-scale and regional-scale simulations were separated. In the site-scale simulation used in this study, the authors hypothesized a flat terrain region with a 5 × 5 grid, and thus, the solar radiation was not affected by topography. Therefore, the simulation of any grid was the same and could be regarded as the representative simulation results of the study region. If the users were only interested in the simulation of a field site experiment or could only provide the input data based on the site/plot scale, then they would not need to provide any information about the topography and stream of their study region which were necessary prepared in the regional-scale simulation. The site-scale simulation, which was used in this study, is convenient for model validation, saves time in terms of model operation, and is easy to use for beginners.

### 2.1.2 Modifications for simulating $NH_3$ volatilization from cultivated uplands

In the original CNMM-DNDC model, the direct processes involved in the calculation of $NH_3$ volatilization from cultivated uplands included ammonium bicarbonate (ABC) decomposition, urea hydrolysis and $NH_3$ volatilization (Fig. S1). Among them, ABC decomposition was regulated by soil pH and soil depth; urea hydrolysis was affected by soil temperature and soil organic carbon; $NH_3$ volatilization from cultivated uplands was simply determined by the regulating factors of wind speed, soil depth and soil temperature (Table S1 and S2). Moreover, other synthetic fertilizers dissolution and organic manure mineralization were involved in the original model. The modifications of the new version of the CNMM-DNDC for simulating $NH_3$ volatilization from cultivated uplands were mainly adapted from Li et al. (2019). Compared to the original CNMM-DNDC, three major modifications were conducted. First, the soil temperature parameter ($f_T$) of the urea hydrolysis function was recalibrated and the effect of soil moisture on urea hydrolysis ($f_{SM}$) was newly added. Second, the regulatory effect of soil temperature on ABC decomposition ($f_{Ts\_ABC}$) was parameterized. Finally, the effects of the original parameters of soil temperature and moisture on $NH_3$ volatilization were recalibrated, and the effects of the clay fraction, plant standing, and canopy wetting on $NH_3$ release to the atmosphere were newly parameterized (Fig. S1). The above-mentioned calibration and parameterization were conducted by Dubache et al. (2019) and Li et al. (2019). Therefore, the $NH_3$ flux from cultivated uplands (flux $(NH_3)_{uplands}$) was jointly determined by the regulating factors of wind speed ($f_{wind}$, 0−1), soil temperature ($f_{temp}$, 0−1), soil moisture ($f_{water}$, 0−1), soil depth ($f_{depth}$, 0−1), clay fraction ($f_{clay}$, 0−1), vegetation canopy ($f_{canopy}$, 0−1), and rainfall-induced canopy wetting ($f_{rain}$, 0−1), as shown in Eq. (1). Each factor was defined as a dimensionless fraction within 0–1. $NH_{3(l)}$ is referred to as the dissolved $NH_3$ in the liquid phase of upland soils. Among these regulating factors, $f_{depth}$ was calculated by the number of soil layers in Li et al. (2019), where the thickness of the soil layer was set as the value of the saturated hydraulic conductivity. However, in the CNMM-DNDC, the simulated soil layers and their corresponding thicknesses were set to be freely defined by users. The algorithm of $f_{depth}$ from Li et al. (2019) was inappropriate for this study. Therefore, $f_{depth}$ was revised using the thickness of the soil layer based on Eq. (2), wherein $d_{soil}$ denotes the depth of the simulated soil layer. The calibration cases with fertilizer application depth were used for the calibration of $f_{depth}$. Moreover, the time step of the CNMM-DNDC was three hours, but the time step was one day in the DNDC model. So the ratio of time steps of the two models ($T_{layer}$ with the value of 8) was involved in Eq. (1). Nevertheless, the deviation between derived from the different time steps existed, as shown in Table S3. To solve the deviation, a time-step parameter ($f_{Tstep}$) was introduced into Eq. (1), which was calculated at 0.75 in this study using the calibration cases with surface broadcast ($n$ = 21). The zero-intercept linear regression was applied for model calibration. We provided the calibration of $f_{Tstep}$ in Fig. S2 as an instance. Table S1 listed the algorithms of the original and modified model in simulating $NH_3$ volatilization from cultivated uplands. The descriptions and units of the symbols used in Table S1 were listed in Table S2.

$$\mathrm{Flux}(\mathrm{NH_3})_{\mathrm{upland}} = 3.6 f_{\mathrm{wind}} f_{\mathrm{temp}} f_{\mathrm{water}} f_{\mathrm{depth}} f_{\mathrm{clay}} f_{\mathrm{canopy}} f_{\mathrm{rain}} f_{\mathrm{Tstep}} \mathrm{NH}_{3(\mathrm{l})} / T_{\mathrm{layer}} \tag{1}$$

$$f_{\mathrm{depth}} = 0.5^{d_{\mathrm{soil}}/0.03} \tag{2}$$

### 2.1.3 Modifications for simulating $NH_3$ volatilization from rice paddy fields

The original CNMM-DNDC failed to simulate $NH_3$ volatilizations from rice paddy fields because it lacked the capability to simulate the surface water-flooded layer over rice paddy fields. Given the presence of floodwater over rice paddy soils, the mechanisms of $NH_3$ volatilization are different between cultivated uplands and rice paddy fields. However, CNMM-DNDC and other widely used biogeochemical models (e.g., DNDC) adopted scientific processes and algorithms applied in simulating $NH_3$ volatilization from fertilized cultivated uplands to calculate $NH_3$ volatilization from rice paddy fields without considering floodwater over soils (Cannavo et al., 2008; Li, 2016). Therefore, floodwater over rice paddy soils was added to the modified CNMM-DNDC. To add this component, the modified CNMM-DNDC adopted the Jayaweera-Mikkelsen model (i.e., J-M model), based on the two-film theory of mass transfer (Jayaweera and Mikkelsen, 1990a), which is one of the most widely applied process-based models for simulating $NH_3$ volatilization from rice paddy fields. The J-M model consists of two processes (Fig. 2): (i) the chemical processes of $NH_4^+$ ions and aqueous $NH_3$ ($NH_{3(aq)}$) equilibrium in floodwater and (ii) the volatilization processes of $NH_{3(aq)}$ transfer in the form of $NH_3$ gas ($NH_{3(air)}$) across the water-air interface to the atmosphere (Rxn1). $k_d$ (first-order, $s^{-1}$) and $k_a$ (second-order, L $mol^{-1}$ $s^{-1}$) are referred to as the dissociation and association rate constants for $NH_4^+/NH_{3(aq)}$ equilibrium, respectively. $k_{vN}$ (first-order, $s^{-1}$) is referred to as the volatilization rate constant of $NH_{3(aq)}$.

$$\mathrm{NH_4^+} \underset{k_\mathrm{a}}{\overset{k_\mathrm{d}}{\rightleftharpoons}} \mathrm{H^+} + \mathrm{NH_{3(aq)}} \xrightarrow{k_\mathrm{vN}} \mathrm{NH_{3(air)}} \tag{Rxn1}$$

According to the above theories, the change rate of the $NH_4^+$ concentration in floodwater ($[NH_4^+]_w$, mol $L^{-1}$) due to $NH_3$ volatilization ($R_a$, mol $L^{-1}$ $s^{-1}$) can be estimated by Eq. (3) as a function of $[NH_4^+]_w$, $H^+$ concentration in floodwater ($[H^+]_w$, mol $L^{-1}$), $k_d$, $k_a$ and $k_{vN}$.

$$R_\mathrm{a} = -\frac{k_\mathrm{d}k_\mathrm{vN}[\mathrm{NH_4^+}]_\mathrm{w}}{k_\mathrm{a}[\mathrm{H^+}]_\mathrm{w} + k_\mathrm{vN}} \tag{3}$$

The dynamic changes in $[H^+]_w$ and $[NH_4^+]_w$ are calculated by the CNMM-DNDC instead of the field experiment described in Jayaweera and Mikkelsen (1990a).

In the modified CNMM-DNDC, the pH of the floodwater, which is the negative logarithm of $[H^+]_w$, is related to the initial pH of water for flooding and that of surface soil. When the floodwater depth is less than 0.04 m, the pH of the floodwater is equal to the mean of the initial pH of water for flooding and that of surface soil, both of which are the inputs of the modified model. Otherwise, the pH of the floodwater is equal to the initial pH of the water for flooding. On the one hand, $[H^+]_w$ is regulated by urea hydrolysis in floodwater, the algorithm of which was derived from that of urea hydrolysis affecting soil pH in the model. On the other hand, many studies have found that a marked diurnal fluctuation in floodwater pH is associated with algal photosynthesis, which was elevated with solar radiation (De Datta, 1995; Fillery and Vlek, 1986). Therefore, a ratio of the daytime solar shortwave radiation effect on algal photosynthesis ($R_{slr}$, 0−1) was established by the authors using Eq. (4) as a quadratic function of the simulation time ($t$, 06:00 to 21:00 with a 3-hour interval) of a day. $R_{slr}$ at the other moments with no or extremely little solar radiation in a day was set as 0. The effect of algal growth ($f_{alg}$) on floodwater pH was calculated by Eq. (5), where the adjusted coefficient ($k_{alg}$, 0−1) was calibrated to 0.75 or 0.6 when the floodwater depth was no more than or more than 0.04 m, respectively. The floodwater pH of ($t$+1)th was modified by the floodwater pH of $t$th and $f_{alg}$ using Eq. 6, which was set as no more than 10.

$$R_{slr} = -0.0036t^2 + 0.1096t - 0.7046 \tag{4}$$

$$f_{alg} = k_{alg} R_{slr} R + 0.25 \tag{5}$$

$$\mathrm{pH}_{t+1} = \mathrm{pH}_t + f_{alg} \tag{6}$$

When fertilizers (e.g., urea) are applied to the rice paddy fields, they are first allocated to the floodwater and soil layers according to the ratio of the floodwater depth and the application depth of fertilizer in the modified CNMM-DNDC. Subsequently, $[NH_4^+]_w$ increases with urea hydrolysis, and ABC decomposition occurs in the floodwater. In the modified model, the calculation of urea hydrolysis in floodwater refers to that in the upland soils (Dubache et al., 2019) by removing the influencing factors of soil organic carbon and soil moisture. Therefore, urea hydrolysis in floodwater is only determined by the floodwater temperature. To simplify the calculation, the floodwater temperature is arbitrarily set equal to the temperature in the first soil layer in the modified model. Given that ABC decomposition in floodwater was not involved in the original CNMM-DNDC, this study directly adopted the algorithm of ABC decomposition in upland soils used in Li et al. (2019), and this process was regulated by soil temperature, pH and the applied depth of fertilizer. However, ABC decomposition in floodwater is different from that in upland soils; i.e., the ABC concentration is uniformly distributed in the floodwater, and the effect factors (i.e., temperature, pH and depth) applied should be those of floodwater rather than those of soil. Therefore, this study ignored the effect of soil depth and retained the effect of floodwater temperature and pH on ABC decomposition in floodwater.

For each simulation time step, the $NH_4^+$ in the floodwater and the first soil layer experiences uniform mixing and exchange. Then, $NH_4^+$ is transported in soil layers, accompanied by organic nitrogen mineralization, consumption via plant uptake, nitrification, volatilization of $NH_3$, and adsorption/desorption by clay (Li, 2016; Li et al., 1992; Li et al., 2019).

$k_d$, $k_a$ and $k_{vN}$ in Eq. (3) are determined by the environmental factors, i.e., the temperature and the depth of floodwater (Jayaweera and Mikkelsen, 1990a). As shown in Eq. (7), $k_a$ is affected by its relationship with floodwater temperature ($T_f$, K) based on Alberty (1983):

$$k_{\mathrm{a}} = 3.8\times10^{11} - 3.4\times10^{9} T_{\mathrm{f}} + 7.5\times10^{6} T_{\mathrm{f}}^{2} \tag{7}$$

$k_d$ is derived from the relationship with the equilibrium constant for $NH_4^+/NH_{3(aq)}$ ($K$) and $k_a$ (Eq. (8)):

$$k_{\mathrm{d}} = K k_{\mathrm{a}} \tag{8}$$

$K$ is calculated as a function of the floodwater temperature (Eq. (9)) derived from Jayaweera and Mikkelsen (1990a):

$$K = 10^{-[0.0897+(2729/T_{\mathrm{f}})]} \tag{9}$$

The $NH_3$ volatilization rate constant ($k_{vN}$) is estimated by the law of conservation of mass, which is considered in the system of $NH_3$ transfer across the air-water interface. By dimensional analysis, $k_{vN}$ is determined by Eq. (10), based on the ratio of the floodwater depth ($d$, m) and the overall mass-transfer coefficient for $NH_3$ ($K_{ON}$, cm $h^{-1}$):

$$k_{\mathrm{vN}} = K_{\mathrm{ON}} \big/ (3.6\times10^{5} d) \tag{10}$$

According to the two-film theory, based on Fick's first law and Henry's law, $K_{ON}$ is determined by Eq. (11) using the exchange constant for $NH_3$ in the gas and liquid phases ($k_{gN}$ and $k_{lN}$, respectively) and the non-dimensional Henry's constant ($H_{nN}$). As described by Jayaweera and Mikkelsen (1990a), $H_{nN}$ is a function of $T_f$, which can be calculated by Eq. (12), whereas $k_{gN}$ and $k_{lN}$ are dependent on the wind speed measured at a height of 8 m ($U_8$, m $s^{-1}$), which can be calculated using Eqs. (13−14). $U_8$ can be determined using the model input of wind speed measured at a height of 10 m ($U_{10}$, m $s^{-1}$), based on Eq. (15) derived from Jayaweera and Mikkelsen (1990a).

$$K_{\mathrm{ON}} = (H_{\mathrm{nN}} k_{\mathrm{gN}} k_{\mathrm{lN}}) \big/ (H_{\mathrm{nN}} k_{\mathrm{gN}} + k_{\mathrm{lN}}) \tag{11}$$

$$H_{\mathrm{nN}} = 183.8e^{(-1229/T_{\mathrm{f}})} \Big/ RT_{\mathrm{f}} \tag{12}$$

$$k_{\mathrm{gN}} = 19.0895 + 742.3016U_8 \tag{13}$$

$$k_{\mathrm{lN}} = \left\{12.5853 \Big/ \left[1 + 43.0565e^{(-0.4417U_8)}\right]\right\} \Big/ 1.6075 \tag{14}$$

$$U_8 = \frac{11.51}{\ln\left(10/8\times10^5\right)} U_{10} \tag{15}$$

Finally, the three-hour cumulative flux of $NH_3$ volatilization (Flux $(NH_3)_{\mathrm{rice}}$, kg N $ha^{-1}$ $3h^{-1}$) is calculated by Eq. (16) using $R_a$, $d$, and the simulation time step based on the molar mass of N (~14 g $mol^{-1}$) and the conversion coefficient from $m^2$ to ha (1 $m^2$ = $1\times10^{-4}$ ha).

$$\mathrm{Flux}\left(\mathrm{NH_3}\right)_{\mathrm{rice}} = -1.512\times10^{9} dR_a \tag{16}$$

The CNMM-DNDC with the above modifications is hereinafter referred to as the modified CNMM-DNDC.

### 2.2 Brief description of the field sites and treatments

Two field observation datasets of $NH_3$ volatilization using micrometeorological methods or wind tunnel techniques, which were measured in cultivated uplands and flooded rice paddy fields of China, respectively, were collected from published peer-reviewed articles. For the dataset of cultivated uplands, the collected field observations were conducted at seven experimental sites, including Dongbeiwang (DBW) in Beijing; Fengqiu with cultivated uplands (FQU) in Henan; Guangchuan (GC) Luancheng (LC), and Quzhou (QZ) in Hebei; Yanting (YT) in Sichuan; and Yongji (YJ) in Shanxi (Fig. 1), and the dataset were directly inherited from Li et al. (2019). The upland sites involved in this study were calcareous soils cultivated with summer maize and winter wheat. The 44 cases of synthetic fertilizer application events in cultivated uplands (Table S4) involved various fertilizer types (including urea, ammonium bicarbonate (ABC), ammonium sulfate, and complex fertilizer), a wide range of applied fertilizer doses (60–348 kg N $ha^{-1}$), and various agricultural management practices (e.g., broadcast or deep point placement of fertilizer(s) alone or fertilization coupled with irrigation). For the rice paddy field dataset, field observations were collected at five experimental sites, including Changshu (CS) and Danyang (DY) in Jiangsu, Fengqiu with rice paddy fields (FQP) in Henan, Shenzhen (SZ) in

Guangdong, and Yingtan (YTA) in Jiangxi (Fig. 1), and these sites were cultivated with summer rice and winter wheat or double rice (Table 1). In total, nineteen (P1–P19) synthetic fertilizer application events were included in these measurements, covering different fertilizer types, including urea and ABC; fertilizer doses in the range of 41–162 kg N $ha^{-1}$; and various agricultural management practices (e.g., broadcasting or broadcasting followed by tillage, Table 1 and Table 2). In addition, the other auxiliary variables, e.g., temperature, pH, and ammonium ($NH_4^+$) concentration of the floodwater, measured in the rice paddy experimental sites during the $NH_3$ volatilization measurement periods were also collected for model calibration and validation.

### 2.3 Model preparation and operation

#### 2.3.1 Input data formatting

The input data of the modified CNMM-DNDC used in this study included the meteorological conditions of the study area (e.g., 3-hourly average air temperature ($T_{\mathrm{air}}$), precipitation ($P$), wind speed ($W$), solar radiation ($R$), relative humidity (RH)), the necessary soil properties of individual layers (e.g., soil clay and sand fraction, organic carbon (SOC), bulk density (BD), pH), crop parameters (e.g., crop type, thermal degree days for maturity (TDD), nitrogen content, plant height and root depth), and the implemented management practices (e.g., plant and harvest dates, methods and/or amounts of individual management practices including fertilization, tillage, irrigation and flooding).

For the meteorological data inputs, the reported 3-hourly meteorological data from the weather station at the experimental site were used. If these data were not available, then data from the adjacent weather station in the China Meteorological Administration (CMA, http://www.data.cma.cn) were adapted by referring to the reported average or maximum values (Table S5, Text S1).

The necessary inputs of surface soil properties at the individual upland sites for the modified model were derived from Li et al. (2019), whereas those at the individual rice paddy sites are shown in Table S6. If the observed surface soil properties were not available, then the values were provided using the methods of Li et al. (2019). The soil clay and sand fraction and pH in the deep layers were set to be consistent with those in the surface soil. Depending on the SOC at the surface soil, the modified

CNMM-DNDC calculated the SOC in the deep layers using the algorithms involved in Li (2016), and the BD in the deep layers were estimated using the SOC value in the corresponding layers based on the algorithms shown in Li (2016). Other soil properties (e.g., field capacity, wilting point and saturated hydraulic conductivity) were estimated using the pedo-transfer functions of Li et al. (2019).

The CNMM-DNDC contains a library of crop parameters. However, to ensure the normal growth of the crop(s), the model's default values for the crop TDD at the individual sites were adapted by the multiyear (at least five years) average of the sums of daily air temperatures during the growing season.

Agricultural management practice information included in the CNMM-DNDC input was organized on a daily scale. The management practice information for the cases of cultivated uplands was derived from Li et al. (2019), whereas that for the cases of rice paddy fields is listed in Table S7. It is worth noting that the information input for the cases of rice paddy fields required the start and end dates of the individual flooding events accompanied by the corresponding pH and depth of floodwater as model inputs. The default value of the initial floodwater pH at all sites was set at 7.0 due to a lack of observations. The cases in DY, FQP and YT had reported floodwater depth observations, and the cases of CS without floodwater depth observations were arbitrarily set to the traditional floodwater depth (0.04 m) of the DY site, which was located in the same region. For the SZ cases without floodwater depth observations, given that no site is adjacent to the Pearl River Delta region where SZ is located, the floodwater depth of the SZ site was calculated at 0.075 m.

### 2.3.2 Model operation

To reduce the influences of initial model inputs, the model simulation consists of a spin-up period conducted for at least five years (depending on the availability of the model inputs) and the corresponding experimental period. The sources of the daily meteorological data for the spin-up period and the following simulation for cultivated uplands and rice paddy field sites were derived from Li et al. (2019) and listed in Table S8, respectively. The cases for model calibration were identified on the basis of covering as many climate conditions, soil properties and management practices as possible. Therefore, for the simulation of $NH_3$ from urea application on cultivated uplands and rice paddy fields, 26 typical cases of DBW, FQU, and QZ and 10 typical cases of DY, FQP, and SZ were used for model calibration. Regarding the simulation of $NH_3$ from the ABC application on cultivated uplands and rice paddy fields, 3 typical cases of DBW and YT and 1 typical DY case were conducted for model calibration. The remaining 23 independent cases were provided for model validation.

### 2.4 Sensitivity analysis

Sensitivity analysis was adopted to investigate model inputs and improved parameters in the modified CNMM-DNDC that simulates $NH_3$ volatilization following fertilizer application. U37 in QZ and P4 in CS were chosen as the baseline cases to assess the model's behavior in simulating $NH_3$ volatilization from cultivated uplands and rice paddy fields, respectively. One reason for this selection was that U37 and P4 were geographically located near the center of the region for cultivated upland and rice paddy cases, respectively. Another reason was that the selected cases implement general Chinese management practices. The authors altered only one item at a time by maintaining the others constant. Meteorological variables (i.e., 3-hourly averages of $T_{air}$ and $W$; 3-hourly totals of $P$ and $R$ during measurement periods of $NH_3$ volatilization), soil properties (i.e., soil clay fraction, pH, SOC content and BD), and field management practices (i.e., water management (irrigation water amount or depth of floodwater) and nitrogen fertilization type, dose and depth) were involved in the sensitivity test of model inputs. The model input items of the 3-hourly average of $W$, 3-hourly totals of $P$ and $R$ during the measurement periods of $NH_3$ volatilization, as well as the soil clay fraction, SOC content, nitrogen fertilization dose, and depth of floodwater, were altered by a range from −30% to +30% with an interval of 10%. Soil BD and pH, with narrow amplitudes in situ, were altered within the ranges of 1.17 to 1.47 (U37) and 0.89 to 1.19 (P4) with an interval of 0.05 and within the ranges of 7.3 to 8.9 (U37) and 6.2 to 8.1 (P4) with an interval of 0.3, respectively. The 3-hourly average $T_{air}$ during the measurement period of $NH_3$ volatilization was altered within the range of −3 ℃ to +3 ℃ with an interval of 1 ℃. The irrigation water amount and nitrogen fertilization depth and type were set as 0.2/0.5/5 cm, 5/10/15 cm and ABC/ammonium-based nitrogen (N) fertilizers excluding ABC, respectively. The corresponding baselines and lower/upper bounds of the above model inputs involved in the sensitivity analysis are listed in Table S9. In addition, the parameters added and revised for simulating $NH_3$ volatilization from cultivated uplands were involved in the sensitivity analysis of improved parameters, including $f_{SM}$ and $f_T$ in the process of urea hydrolysis, $f_{Ts\_ABC}$ in the process of ABC decomposition, and $f_{temp}$, $f_{clay}$, $f_{water}$, $f_{depth}$, $f_{canopy}$ and $f_{rain}$ in the process of liquid $NH_3$ volatilization. The parameters in Eq. (3) for simulating $NH_3$ volatilization from rice paddy fields were involved in the sensitivity analysis of improved parameters, including $k_d$, $k_a$ and $k_{vN}$. And $f_{alg}$, a newly introduced factor effect on floodwater pH, was also involved in the sensitivity analysis of improved parameters for simulating $NH_3$ volatilization from rice paddy fields. In each sensitivity analysis, an improved parameter was altered by a range from −30% to +30% by an interval of 10%, with the others remaining constant. The sensitivity analysis of $f_{Ts\_ABC}$ was conducted at U4 case in QZ with ABC application. The change ratios of cumulative $NH_3$ volatilization during the measurement periods between the lower/upper and baseline simulations were applied as the quantitative evaluation index for the sensitivity analysis (Abdalla et al., 2020).

### 2.5 Evaluation of model performance and statistical analysis

The index of agreement (IA), Nash–Sutcliffe Index (NSI), relative model bias (RMB), as well as slope, significance level and coefficient of determination ($R^2$) of the zero-intercept linear regression (ZIR) between the observed (*O*) and simulated (*S*) values were applied to quantitatively assess the performance of the original and modified models. The algorithms of these statistical metrics refer to Li et al. (2019). If the slope and $R^2$ of the zero-intercept linear regression as well as the IA and NSI values are closer to 1, then the model performance is better. The SPSS Statistics Client 19.0 (SPSS Inc., Chicago, USA) software package was used for the multiple regression analysis. The Origin 8.0 (OriginLab Ltd., Guangzhou, China) software package was used for graph drawing.

## 3. Results

### 3.1 Ammonia volatilization from cultivated uplands

The observed cumulative $NH_3$ volatilization (CAV) in all the cases of cultivated uplands during the measurement periods totaled 0.6–127.7 kg N ha$^{-1}$ (mean: 27.5 kg N ha$^{-1}$). The corresponding CAVs simulated by the original and modified CNMM-DNDC totaled 0.5–94.1 kg N ha$^{-1}$ (mean: 33.2 kg N ha$^{-1}$) and 0.8–115.2 kg N ha$^{-1}$ (mean: 27.8 kg N ha$^{-1}$), respectively (Table S4). The original

CNMM-DNDC performed poorly in simulating all the observed cumulative $NH_3$ volatilization cases, showing an acceptable IA (0.55), an unacceptable NSI (–1.49) and an insignificant ZIR (slope = 1.11 and $R^2$ = 0.06) (data not shown).

In this study, several modifications were conducted to improve the CNMM-DNDC performance in simulating $NH_3$ volatilizations from cultivated uplands. Regarding either the typically calibrated or independently validated cases, the modified CNMM-DNDC did not perform well in simulating daily $NH_3$ fluxes, with low IA and unacceptable NSI values (Table 3). This result was probably because the simulated $NH_3$ dynamic peak time could not absolutely be matched to the observed peak time, although the modified model captured the observed $NH_3$ dynamic trend. For the 3 only typically calibrated ABC cases, the modified model performed marginally well in simulating CAVs, showing a good IA (0.75) but a low NSI (0.14) and an insignificant ZIR ($R^2$ = 0.64) (Table 3). However, the modified model showed a perfect performance in simulating CAVs of both the calibrated and validated urea cases, with IA values (0.93 and 0.91) close to 1, acceptable NSI values (0.73 and 0.49), and significant ZIRs ($R^2$ = 0.71 with slope = 0.94 and $R^2$ = 0.74 with slope = 1.06) (Table 3). Regarding the CAVs of all the individual cases of cultivated uplands, the modified model reported an |RMB| of 1.0–307.8% (mean: 69.8%, Table 2), with only 16% (seven of forty-four) of cases suffering from an |RMB| larger than 100%.

### 3.2 Ammonia volatilization from rice paddy fields

Figure 3, 4 and 5 illustrated the observed and simulated $NH_3$ volatilization and auxiliary variables (e.g., temperatures, pH and $NH_4^+$ concentrations of floodwater) in each rice paddy case. The cases with the same observed variables were associated in a figure for unified formatting. The observed CAVs in all cases of rice paddy fields (2 and 17 cases for ABC and urea applications, respectively) during the measurement periods totaled 5.9–39.8 kg N $ha^{-1}$ (mean: 18.1 kg N $ha^{-1}$, Table 2), with fertilizer application doses of 40.5–162.2 kg N $ha^{-1}$ (mean: 81.4 kg N $ha^{-1}$). Given the lack of the capacity to simulate the water-flooded layer over rice paddy fields, the original CNMM-DNDC could not simulate $NH_3$ volatilizations from rice paddy fields. The corresponding CAVs simulated by the modified CNMM-DNDC totaled 3.4–39.1 kg N $ha^{-1}$ (mean: 16.2 kg N $ha^{-1}$, Table 2). Regarding the CAVs of all the individual cases of rice paddy fields, the modified model demonstrated an |RMB| of 0.3–94.9% (mean: 32.7%, Table 2), and none of nineteen cases showed an |RMB| larger than 100%. With regard to the only two ABC cases, the simulated daily $NH_3$ fluxes generally matched the observations of the typically calibrated and independently validated cases (P1 and P2, respectively), although the simulated peak emissions of the first day for P1 were lower than the observations (Fig. 3e–f). For P1 and P2, the corresponding statistical indices showed that IA values were 0.33 and 0.94, the NSI values were 0.02 and 0.85, and the ZIR slopes were 0.16 (not available $R^2$ and $p$ values, $n$ = 7) and 0.90 ($R^2$ = 0.71, not significant, $n$ = 4), respectively (Table 3). The observed and simulated daily $NH_3$ fluxes due to urea application in the individual cases are illustrated in Fig. 4c–f and Fig.5i–k, respectively. As the figures demonstrate, the temporal $NH_3$ flux variation pattern simulated by the modified model generally followed that observed in the field. Regarding the simulations of the 10 typically calibrated and 7 independently validated urea cases, the modified model did not show good performance in terms of the daily $NH_3$ flux, with IA values of 0.53 and 0.72, NSI values of –0.35 and 0. 36 and ZIR slopes of 0.47 ($R^2$ = 0.04, $p$ < 0.05, $n$ = 176) and 0.56 ($R^2$ = 0.19, $p$ < 0.001, $n$ = 63), respectively (Table 3). However, the modified CNMM-DNDC performed extremely well in simulating CAVs of the calibrated and validated urea cases, showing good IA values of 0.88 and 0.85, acceptable NSI values of 0.30 and 0.60, and significant ZIR slopes of 1.03 ($R^2$ = 0.68, $n$ = 10) and 0.77 ($R^2$ = 0.65, $n$ = 7), respectively (Table 3).

### 3.3 Model performance in terms of other auxiliary variables in rice paddy fields

Table 4 lists the statistical indices used to evaluate the performance of the modified CNMM-DNDC in the simulation of floodwater temperatures, pH values and $NH_4^+$ concentrations when the model was calibrated and validated. The modified model generally captured the trends in floodwater temperature (Fig. 5a–b), although the simulated floodwater temperatures of several certain days for P9 were lower than the observations. The modified CNMM-DNDC, which introduced the effect of algal growth on floodwater pH, generally simulated the observed daily elevated floodwater pH resulting from algal photosynthetic activity (Fig. 3a–b and Fig. 5c–e). The simulation of calibrated (P1, P9 and P10, Fig. 3a and Fig. 5c–d) and validated cases (P2 and P19, Fig. 3b and Fig. 5e) of floodwater pH resulted in good IA values of 0.83 and 0.79, acceptable NSI values of 0.55 and 0.36, and ZIRs with significant $R^2$ values of 0.55 (slope = 1.00, $n$ = 147) and 0.36 (slope = 1.01, $n$ = 45), respectively. The simulated and observed daily $NH_4^+$ concentrations in the floodwater of the ABC and urea cases are illustrated in Fig. 3c–d, Fig. 4a–b and Fig. 5f–h. Compared to the observed floodwater $NH_4^+$ concentrations of the ABC cases, the model simulation underestimated the peak concentration on the first day after ABC application for the P1 case but captured the peak concentration of the P2 case (Fig. 3c–d). The modified CNMM-DNDC generally captured the observed temporal pattern in the daily $NH_4^+$ concentrations during the observation periods following urea application, although discrepancies existed in the magnitudes of some cases; e.g., the model overestimated the floodwater $NH_4^+$ concentration in the P7 and P8 cases (Fig. 4a–b) and underestimated that in the P6 (Fig. 4b) and P19 cases (Fig. 5h). Significant ZIRs between the simulated and observed daily floodwater $NH_4^+$ concentrations of the typically calibrated and independently validated cases yielded significant slopes of 1.03 ($R^2$ = 0.48, $n$ = 24) and 0.74 ($R^2$ = 0.34, $n$ = 55), the IA values were 0.78 and 0.68, and the NSI values were 0.48 and 0.25, respectively (Table 4).

### 3.4 Summary for the performance of CNMM-DNDC in simulating $NH_3$ volatilization

To sum up, as Fig. 6 shows, with regard to the simulations of all 40 typically calibrated and 23 independently validated cases of cultivated uplands and rice paddy fields by the modified model, significant zero-intercept linear relationships between the simulated and observed CAVs were found, with slopes of 0.94 ($R^2$ = 0.76) and 0.98 ($R^2$ = 0.71), respectively. In general, the above results indicated that the modifications made in this study obviously improved the performance of the CNMM-DNDC in simulating $NH_3$ volatilization following applications of synthetic nitrogen fertilizers to cultivated upland and rice paddy soils. Nevertheless, the simulated CAV from cultivated upland cases with fertilizer application depth (U6, U20 and U44) and irrigation/precipitation (U16, U22 and U26) by the modified model resulted in the RMB larger than 150%. With regard to the cases in the rice paddy fields, the simulations of the modified model with an absolute value of RMB larger than 50% occurred in P1, P9 and P13 cases. The modified model resulted in the largest RMB of 94.9% between the observed and simulated CAV occurred in the urea case of P9 which was located in DY under cloudy conditions. The ABC case of P1 with RMB of –57% suffered from a seriously underestimation of $NH_4^+$ concentration in the floodwater (Fig. 3). For the cases in SZ, the modified CNMM-DNDC generally underestimated $NH_3$ volatilization from the almost all cases with low N dose, but overestimated $NH_3$ volatilization from the cases with high N dose.

### 3.5 Sensitivity of model inputs and improved parameters in simulating $NH_3$ volatilization

The sensitivity analysis of model input items indicated that $NH_3$ volatilization from cultivated uplands was primarily regulated by field management practices (Fig. 7a). The changes in N dose, the different N types and the implementation of irrigation had considerable effects on $NH_3$ volatilization from cultivated uplands. In addition, a fertilization depth of 15 cm resulted in a –23% change in $NH_3$ volatilization, and the increase in irrigation amount had an inhibitory effect on $NH_3$ volatilization. Moreover, in comparison to other soil properties, the changes in soil SOC had a greater influence (–19% to 16%) on $NH_3$ volatilization. Among all considered meteorological variables, $NH_3$ volatilization from cultivated uplands appeared to be the most sensitive response to changes in air temperature (Fig. 7a). However, $NH_3$ volatilization from rice paddy soils was sensitive to changes in fertilization and floodwater management, which increased with N dosage and decreased with the depth of fertilizer application and that of floodwater (Fig. 7b). For all soil variables considered in the sensitivity analysis, only the changes in soil pH had a great influence on $NH_3$ volatilization from rice paddy fields. In addition, $NH_3$ volatilization from rice paddy soils decreased with solar radiation. With regard to the sensitivity analysis of the improved parameters, $NH_3$ volatilization from cultivated uplands showed more sensitive to the reduction of the improved parameters than to the increase of those. Generally, as the improved parameters reduced, $NH_3$ volatilization from cultivated uplands decreased. Moreover, $NH_3$ volatilization from rice paddy fields displayed complicated response to the change of the improved parameters involved in the process of $NH_3$ volatilization from rice paddy fields. For instance, no matter whether $k_a$ increased or reduced, $NH_3$ volatilization trend to decrease while $NH_3$ volatilization increased with the increasing of $k_d$. The above results indicated that the modifications in simulating $NH_3$ volatilization from either cultivated uplands or rice paddy fields were effective and feasible.

## 4. Discussion

### 4.1 Model performance in simulating $NH_3$ volatilization from cultivated uplands

The mechanism of $NH_3$ volatilization in the modified CNMM-DNDC is mainly inherited from that in the DNDC model modified by Li et al. (2019). The simulated rate of $NH_3$ flux is jointly determined by the regulating factors of wind speed, soil depth, clay fraction, soil temperature, soil moisture, vegetation canopy, and rainfall-induced canopy wetting. We found that the complicated management practices bring obstacles to modeling. Across all the cases of cultivated uplands (Table S4), the simulations of the modified CNMM-DNDC with an RMB larger than 150% occurred in the cases with fertilizer application depth (U6 with broadcast followed by tillage (BFT) 20 cm, U20 with BFT 5 cm and U44 with deep point placement 5–10 cm) and irrigation/precipitation (U16 with 4–6 cm irrigation, U22 with 4–6 cm irrigation and U26 with 0.8 cm irrigation and 3.69 cm precipitation). Among the all cases with fertilizer application depth or irrigation/precipitation (including 38 cases), the proportion of the cases with RMB greater than 150% accounted for 16% (6 cases). This result might be because the model could not simulate well the inhibition mechanisms of some situations of fertilization depth and water-adding events effect on $NH_3$ volatilization. Moreover, Li et al. (2019) also reported that irrigation/precipitation during the measurement periods had a complex effect (e.g., reduction and stimulation) on $NH_3$ volatilization following nitrogen fertilizer application in cultivated uplands, and determining this information is still a considerable challenge in $NH_3$ simulations by biogeochemical models. At the same time, Li et al. (2019) also found that the doses and depths of the fertilizer applications jointly accounted for 43% ($p < 0.001$) of the variance in the observed CAVs. The results demonstrated that the simulated $NH_3$ volatilization from cultivated uplands following nitrogen fertilizer application accompanied with deep- or mixed-placement or irrigation/precipitation by the modified model still had some deviation from the observations, and more synchronous observations of $NH_3$ volatilization and other auxiliary variables (e.g., soil moisture, $NH_4^+$ concentration and nitrogen uptake by crops) in these situations are urgently needed to further revise the CNMM-DNDC.

### 4.2 Model performance in simulating $NH_3$ volatilization from rice paddy fields

In this study, four improvements in the pH of floodwater were involved in the modified

CNMM-DNDC. First, floodwater over rice paddy soil was added, which enabled the simulation of floodwater pH in the modified model. Second, the modified model used the initial pH of floodwater and the pH of the surface soil to calculate the floodwater pH. The above two improvements allowed the introduction of the J-M model into the modified CNMM-DNDC. The present relatively reliable biogeochemical models rarely involve floodwater over rice paddy soil when simulating $NH_3$ volatilization from rice paddy fields, which is not in accordance with the natural state. Third, when urea was applied to the surface floodwater, the subsequent urea hydrolysis reaction could increase the floodwater pH, and this process was added to the modified model by referring to the algorithms applied in the original model for upland soils (Sec. 2.1.2). Finally, the effect of algal growth on floodwater pH was introduced into the modified model by calculating the ratio of the solar shortwave radiation effect on algal photosynthesis. In detail, under cloudy conditions in DY (P9), only 9% of the applied urea-N was observed to be lost as $NH_3$ from the rice paddy soil, while up to 40% of the applied urea-N was observed to be lost under high solar radiation conditions in YTA (P19) (Cai et al., 1992). However, the modified CNMM-DNDC overestimated the emissions from DY but underestimated those from YTA, which could be attributed to the overestimation of the pH during the first three observation days in DY and the underestimation of $NH_4^+$ concentrations in YTA (Fig. 5). In addition, algal blooms only appeared on the surface of calm water; thus, a number of factors, such as irrigation, heavy rain, strong wind, and drainage, could hamper the growth of algae (Cao et al., 2013). Due to the basal dressing followed by irrigation (Gong et al., 2013), which inhibited the reproduction of algae in SZ (P11 and P12 cases), the observed $NH_3$ emissions accounted for only 10%−13% of the applied nitrogen. Unfortunately, the aforementioned factors that reduced algal growth were not introduced into the modified CNMM-DNDC because of limited reports, which resulted in an overestimation of $NH_3$ emissions of 6.4 and 2.6 kg N $ha^{-1}$ for P11 and P12 in SZ cases with a high rate of urea application, respectively. More observational data on the effect of algal growth on floodwater pH and subsequent $NH_3$ volatilization are needed to improve the simulation of the modified model on $NH_3$ volatilization from rice paddy fields. Therefore, the modified CNMM-DNDC with the introduction of a floodwater layer, as well as the corresponding processes, into the simulation of $NH_3$ volatilization provided a more scientific algorithm for the simulation of $NH_3$ loss from rice paddy fields, thereby enabling the simulation of the pH and

$NH_4^+$ concentration of floodwater. However, the depth of surface floodwater was kept at a constant value (such as the average depth of the floodwater) for each flooding event in the modified model, but this operation was inconsistent with the field states. The floodwater depth actually changed with real-time evaporation and precipitation. Therefore, a module for calculating the dynamics of floodwater depth driven by real-time evaporation and precipitation is needed to better simulate the effect of floodwater depth on $NH_3$ volatilization. The results of this study suggest that accurate field measurements and a corresponding reliable simulation of floodwater depth are crucial for the simulation of $NH_3$ volatilization by the modified CNMM-DNDC.

### 4.3 Differences between $NH_3$ volatilization from cultivated uplands and rice paddy fields

$NH_3$ volatilization from soil-plant upland systems is an extremely complex process (Freney and Simpson, 1983; Sommer et al., 2004). It is obvious that soil properties play an important role in regulating $NH_3$ volatilization from cultivated uplands, as has been reported by a great number of studies (e.g., Duan and Xiao, 2000; Lei et al., 2017; Martens and Bremner, 1989). In addition, $NH_3$ volatilization from cultivated uplands was simultaneously regulated by the complicated management practices. As the sensitivity analysis indicated, $NH_3$ volatilization from cultivated uplands was primarily regulated by the dose, type and application depth of N fertilizer and water management (Fig. 7a). With regard to $NH_3$ volatilization from rice paddy fields , floodwater pH has been considered one of the primary factors affecting $NH_3$ volatilization from rice paddy fields (Fillery et al., 1984; Hayashi et al., 2006; Jayaweera and Mikkelsen, 1991). As floodwater pH increases, the equilibrium of $NH_4^+$ ions and $NH_{3(aq)}$ in floodwater transfers in the direction of $NH_{3(aq)}$ formation, which will increase the potential for subsequent $NH_3$ volatilization (Jayaweera and Mikkelsen, 1990a; Sommer et al., 2004). Previous studies have also shown that the stimulation of $NH_3$ volatilization from rice paddy fields is affected by algal growth, which largely contributes to the elevation of floodwater pH resulting from algal photosynthetic activity (Buresh et al., 2008; Fillery and Vlek, 1986; Mikkelsen et al., 1978). The addition of a suitable photosynthetic inhibitor also controlled the pH of the floodwater, implying that the increase in pH was caused by algal growth (Bowmer and Muirhead, 1987). In addition, many studies have found that the depth of surface floodwater has a substantial influence on $NH_3$ volatilization (Fillery et al., 1984; Freney et al., 1988; Hayashi et al., 2006). The sensitivity analysis of this study also indicated that $NH_3$ volatilization from rice paddy fields was sensitive to changes in the depth of surface floodwater (Fig. 7b). Jayaweera and Mikkelsen (1990b) demonstrated that the volatilization rate of $NH_3$ decreases as the depth of floodwater increases despite the small difference in meteorological factors and soil physicochemical properties. The reducing effects might be attributed to the following mechanisms. First, with increasing floodwater depth, the concentration of $NH_4^+$ in floodwater decreases (Cai et al., 1986). Many studies have found that a lower concentration of $NH_4^+$ in floodwater contributes to the reduced potential of $NH_3$ volatilization in paddy fields (Bhagat et al., 1996; Hayashi et al., 2006; He et al., 2014; Liu et al., 2015; Song et al., 2004). Observations based on wind-tunnel experiments showed that the $NH_3$ loss decreased from 14.6 mg $L^{-1}$ to 4.5 mg $L^{-1}$ as the depth of floodwater increased from 6.4 cm to 21.3 cm, while other environmental conditions were similar (Jayaweera et al., 1990). Second, a reduction in the depth of floodwater increases the volatilization rate constant of $NH_{3(aq)}$ ($k_{vN}$), thus increasing $NH_3$ volatilization from floodwater.

According to the above results, the regulatory factors affecting $NH_3$ volatilization from rice paddy fields were demonstrated to be different from those from cultivated uplands, which was also supported by previous research (Tian et al., 2001; Zhao et al., 2009). $NH_3$ volatilization from cultivated uplands was primarily influenced by the regulatory factors of soil properties and field management practices. However, given the existence of floodwater over rice paddy field soils, $NH_3$ volatilization from rice paddy fields was additionally affected by flooding management strategies, such as floodwater pH and depth. Therefore, the mechanisms and algorithms applied in simulating $NH_3$ volatilization from cultivated uplands are not appropriate for simulating $NH_3$ volatilization from rice paddy fields. In the modified CNMM-DNDC, $NH_3$ volatilization following nitrogen fertilizer application in cultivated uplands was based on first-order kinetics. However, the modified CNMM-DNDC adopted the J-M model, which was based on the two-film theory of mass transfer, to calculate $NH_3$ volatilization following nitrogen fertilizer application in rice paddy field soils. The results suggest that the application of two different mechanisms according to the distinguished properties of cultivated uplands and rice paddy fields to simulate $NH_3$ volatilization is necessary for process-based biogeochemical models, such as the CNMM-DNDC used in this study.

## Conclusions

The Catchment Nutrient Management Model-DeNitrification-DeComposition (CNMM-DNDC) model was evaluated and modified based on 44 and 19 field observation cases of ammonia ($NH_3$) volatilization following synthetic fertilizer application events in cultivated uplands and rice paddy fields in China, respectively. The original CNMM-DNDC performed poorly in terms of simulating the observed $NH_3$ volatilizations from cultivated uplands, and it failed to simulate $NH_3$ volatilization from rice paddy fields because it could not simulate the water-flooded layer over the rice paddy field. The mechanisms of $NH_3$ volatilization from cultivated uplands and rice paddy fields are different due to the existence of floodwater over rice paddy soils. Therefore, separate modules simulating $NH_3$ volatilization from uplands and rice paddy fields were developed. The primary modifications for simulating $NH_3$ volatilization from cultivated uplands were mainly adopted from Li et al. (2019), and $NH_3$ volatilization from cultivated uplands are regulated by meteorological conditions, soil properties and crop statuses. With regard to the simulation of $NH_3$ volatilization from rice paddy fields, four major modifications were performed in this study. First, floodwater over rice paddy soil, as well as the simulation of floodwater pH, was added to the module simulating $NH_3$ volatilization from rice paddy fields. Second, the Jayaweera-Mikkelsen model was newly introduced into the modified CNMM-DNDC to calculate $NH_3$ volatilization from rice paddy fields. Third, the effect of algal growth on floodwater pH was newly parameterized and added into the model. Finally, the parameters corresponding to $NH_3$ volatilization following ammonium bicarbonate application were calibrated. The modified model provided an excellent performance in simulating $NH_3$ volatilization following synthetic nitrogen fertilizer applications to either cultivated uplands or rice paddy fields. The sensitivity analysis demonstrated that $NH_3$ volatilization from cultivated uplands was principally regulated by soil properties and field management practices while fertilizer application and flooding management strategies, such as floodwater pH and depth, played a major role in regulating $NH_3$ volatilization from rice paddy fields.

*Data availability.* All of the model output used to produce the figures can be obtained from the Supplement, and all of the observed data sets used in this study were collected from published peer-reviewed articles. The code and executive program of the modified model can be obtained from http://doi.org/10.6084/m9.figshare.19388756.

*Author contribution.* XZ, YL, and WZ contributed to developing the idea and methodology of this study. SL arranged the research data, improved and implemented the model simulation, prepared the paper with contributions from all co-authors. RW, KW, and CZ contributed to collect and maintained the research data. SH, CL, and ZY analyzed study data and verified the results.

*Competing interests.* The authors declare that they have no conflict of interest.

*Acknowledgments.* This work was supported by the Chinese Academy of Sciences (grant numbers: ZDBS-LY-DQC007), the National Natural Science Foundation of China (grant numbers: 41907280) and the China Postdoctoral Science Foundation (grant numbers: 2019M650808).

**References**

Abdalla, M., Song, X., Ju, X., Topp, C. F. E., Smith, P.: Calibration and validation of the DNDC model to estimate nitrous oxide emissions and crop productivity for a summer maize-winter wheat double cropping system in Hebei, China, Environ. Pollut., 262, doi:10.1016/j.envpol.2020.114199, 2020.

Alberty, R. A.: Physical chemistry, John Wiley & Sons, New York, 1983.

Anderson, D. M., Burkholder, J. M., Cochlan, W. P., Glibert, P. M., Gobler, C. J., Heil, C. A., Kudela, R. M., Parsons, M. L., Rensel, J. E. J., Townsend, D. W., Trainer, V. L., Vargo, G. A.: Harmful algal blooms and eutrophication: Examining linkages from selected coastal regions of the United States, Harmful Algae, 8, 39–53, doi:10.1016/j.hal.2008.08.017, 2008.

Behera, S. N., Sharma, M., Aneja, V. P., Balasubramanian, R.: Ammonia in the atmosphere: a review on emission sources, atmospheric chemistry and deposition on terrestrial bodies, Environ. Sci. Pollut. R., 20, 8092–8131, doi:10.1007/s11356-013-2051-9, 2013.

Bhagat, R. M., Bhuiyan, S. I., Moody, K.: Water, tillage and weed interactions in lowland tropical rice: a review, Agr. Water Manage., 31, 165–184, doi:10.1016/0378-3774(96)01242-5, 1996.

Bobbink, R., Hornung, M., Roelofs, J. G. M.: The effects of air-borne nitrogen pollutants on species diversity in natural and semi-natural European vegetation, J. Ecol., 86, 717–738, doi:10.1046/j.1365-2745.1998.8650717.x, 1998.

Bouwman, A. F., Lee, D. S., Asman, W. A. H., Dentener, F. J., VanderHoek, K. W., Olivier, J. G. J.: A global high-resolution emission inventory for ammonia, Global Biogeochem. Cy., 11, 561–587, doi:10.1029/97gb02266, 1997.

Bowmer, K. H., Muirhead, W. A.: Inhibition of algal photosynthesis to control pH and reduce ammonia volatilization from rice floodwater, Fertil. Res., 13, 13–29, doi:10.1007/BF01049799, 1987.

Buresh, R., Ramesh Reddy, K. and van Kessel, C.: Nitrogen Transformations in Submerged Soils, In: Raun, J.S.S.a.W.R. editor, Nitrogen in Agricultural Systems, 401–436, 2008.

Cai, G., Peng, G., Wang, X., Zhu, J.: Ammonia volatilization from urea applied to acid paddy soil in southern china and its control, Pedosphere, 2, 345–354, 1992.

Cai, G., Zhu, Z., Trevitt, A., Freney, J. R., Simpson, J. R.: Nitrogen loss from ammonium bicarbonate and urea fertilizers applied to flooded rice, Fertil. Res., 10, 203–215, doi:10.1007/BF01049350, 1986.

Cannavo, P., Recous, S., Parnaudeau, V., Reau, R.: Modeling N dynamics to assess environmental impacts of cropped soils, Advances in Agronomy, 97, Academic Press, 131–174, 2008.

Cao, Y., Tian, Y., Yin, B., Zhu, Z.: Proliferation of algae and effect of its on fertilizer–N immobilization in flooded paddy field, J. Plant Nutr. Fertil. Sc., 19, 111–116, doi:10.11674/zwyf.2013.0113, 2013.

Chien, S. H., Prochnow, L. I., Cantarella, H.: Chapter 8 Recent developments of fertilizer production and use to improve nutrient efficiency and minimize environmental impacts, Advances in Agronomy, 102, Academic Press, 267–322, 2009.

De Datta, S. K.: Nitrogen transformations in wetland rice ecosystems, Fertil. Res., 42, 193–203, doi:10.1007/bf00750514, 1995.

Duan, Z., Xiao, H.: Effects of soil properties on ammonia volatilization, Soil Sci. Plant Nutr., 46, 845–852, 2000.

Dubache, G., Li, S., Zheng, X., Zhang, W., Deng, J.: Modeling ammonia volatilization following urea application to winter cereal fields in the United Kingdom by a revised biogeochemical model, Sci. Total

Environ., 660, 1403–1418, doi:10.1016/j.scitotenv.2018.12.407, 2019.

Dutta, B., Congreves, K. A., Smith, W. N., Grant, B. B., Rochette, P., Chantigny, M. H., Desjardins, R. L.: Improving DNDC model to estimate ammonia loss from urea fertilizer application in temperate agroecosystems, Nutr. Cycl. Agroecosys., 106, 275–292, doi:10.1007/s10705-016-9804-z, 2016.

Felix, J. D., Elliott, E. M., Gish, T. J., McConnell, L. L., Shaw, S. L.: Characterizing the isotopic composition of atmospheric ammonia emission sources using passive samplers and a combined oxidation-bacterial denitrifier approach, Rapid Commun. Mass Sp., 27, 2239–2246, doi:10.1002/rcm.6679, 2013.

Fillery, I. R. P., Simpson, J. R., Dedatta, S. K.: Influence of field environment and fertilizer management on ammonia loss from flooded rice, Soil Sci. Soc. Am. J., 48, 914–920, doi:10.2136/sssaj1984.03615995004800040043x, 1984.

Fillery, I. R. P., Vlek, P. L. G.: 4. Reappraisal of the significance of ammonia volatilization as an N loss mechanism in flooded rice fields, Fertil. Res., 9, 79–98, doi:10.1007/BF01048696, 1986.

Freney, J. R., Simpson, J. R.: Gaseous loss of nitrogen from plant-soil systems, Developments in plant and soil sciences, 9, 1983.

Freney, J. R., Trevitt, A. C. F., Muirhead, W. A., Denmead, O. T., Simpson, J. R., Obcemea, W. N.: Effect of water depth on ammonia loss from lowland rice, Fertil. Res., 16, 97–107, doi:10.1007/bf01049767, 1988.

Giltrap, D., Saggar, S., Rodriguez, J., Bishop, P. :Modelling $NH_3$ volatilisation within a urine patch using NZ-DNDC, Nutr. Cycl. Agroecosys., 108, 267–277, doi:10.1007/s10705-017-9854-x, 2017.

Gong, W., Zhang, Y., Huang, X., Luan, S.: High–resolution measurement of ammonia emissions from fertilization of vegetable and rice crops in the Pearl River Delta Region, China, Atmos. Environ., 65, 1–10, doi:10.1016/j.atmosenv.2012.08.027, 2013.

Han, K., Zhou, C., Wang, L.: Reducing ammonia volatilization from maize fields with separation of nitrogen fertilizer and water in an alternating furrow irrigation system, J. Integr. Agr., 13, 1099–1112, doi:10.1016/s2095-3119(13)60493-1, 2014.

Hayashi, K., Nishimura, S., Yagi, K.: Ammonia volatilization from the surface of a Japanese paddy field during rice cultivation, Soil Sci. Plant Nutr., 52, 545–555, doi:10.1111/j.1747-0765.2006.00053.x, 2006.

He, Y., Yang, S., Xu, J., Wang, Y., Peng, S.: Ammonia volatilization losses from paddy fields under controlled irrigation with different drainage treatments, Sci. World J., doi:10.1155/2014/417605, 2014.

Holcomb III, J. C., Sullivan, D. M., Horneck, D. A., Clough, G. H.: Effect of irrigation rate on ammonia volatilization, Soil Sci. Soc. Am. J., 75, 2341–2347, doi:10.2136/sssaj2010.0446, 2011.

Huang, X., Song, Y., Li, M., Li, J., Huo, Q., Cai, X., Zhu, T., Hu, M., Zhang, H.: A high-resolution ammonia emission inventory in China, Global Biogeochem. Cy., 26, GB1030, doi:10.1029/2011gb004161, 2012.

Jayaweera, G. R., Mikkelsen, D. S.: Ammonia volatilization from flooded soil systems - a computer-model. I. Theoretical aspects, Soil Sci. Soc. Am. J., 54, 1447–1455, doi:10.2136/sssaj1990.03615995005400050039x, 1990a.

Jayaweera, G. R., Mikkelsen, D. S.: Ammonia volatilization from flooded soil systems - a computer-model. II. Theory and model results, Soil Sci. Soc. Am. J., 54, 1456–1462, doi:10.2136/sssaj1990.03615995005400050040x, 1990b.

Jayaweera, G. R., Mikkelsen, D. S.: Assessment of ammonia volatilization from flooded soil systems, Adv. Agron., 45, 303–356, doi:10.1016/S0065-2113(08)60044-9, 1991.

Jayaweera, G. R., Paw U., K. T., Mikkelsen, D. S.: Ammonia volatilization from flooded soil systems: a computer model. III. Validation of the model, Soil Sci. Soc. Am. J., 54, 1462–1468, doi:10.2136/sssaj1990.03615995005400050041x, 1990.

Kong, L., Tang, X., Zhu, J., Wang, Z., Pan, Y., Wu, H., Wu, L., Wu, Q., He, Y., Tian, S., Xie, Y., Liu, Z., Sui, W., Han, L., Carmichael, G.: Improved inversion of monthly ammonia emissions in China based on the Chinese ammonia monitoring network and ensemble Kalman filter, Environ. Sci. Technol., 53, 12529–12538, doi:10.1021/acsest.9b02701, 2019.

Lei, T., Guo, X., Ma, J., Sun, X., Feng, Y., Wang, H.: Kinetic and thermodynamic effects of moisture content and temperature on the ammonia volatilization of soil fertilized with urea, Int. J. Agr. Biol. Eng., 10, 134–143, doi:10.25165/j.ijabe.20171006.3232, 2017.

Li, C.: Biogeochemistry: Scientific fundamentals and modelling approach, Tsinghua University Press, Beijing, 2016.

Li, C., Frolking, S., Frolking, T. A.: A model of nitrous-oxide evolution from soil driven by rainfall events. 1. Model structure and sensitivity, J. Geophys. Res. - Atmos., 97, 9759–9776, doi:10.1029/92jd00509, 1992.

Li, H., Han, Y., Cai, Z.: Modeling the ammonia volatilization from common urea and controlled releasing urea fertilizers in paddy soil of Taihu region of China by Jayaweera–Mikkelsen model, Environ. Sci., 29, 1045–1052, doi:10.1007/BF01049507, 2008.

Li, S., Zheng, X., Zhang, W., Han, S., Deng, J., Wang, K., Wang, R., Yao, Z., Liu, C.: Modeling ammonia volatilization following the application of synthetic fertilizers to cultivated uplands with calcareous soils using an improved DNDC biogeochemistry model, Sci. Total Environ., 660, 931–946, doi:10.1016/j.scitotenv.2018.12.379, 2019.

Li, Y., Schichtel, B. A., Walker, J. T., Schwede, D. B., Chen, X., Lehmann, C. M. B., Puchalski, M. A., Gay, D. A., Collett, J. L., Jr.: Increasing importance of deposition of reduced nitrogen in the United States, P. Nat. Acad. Sci., USA 113, 5874–5879, doi:10.1073/pnas.1525736113, 2016.

Li, Y., Shen, J., Wang, Y., Gao, M., Liu, F., Zhou, P., Liu, X., Chen, D., Zou, G., Luo, Q., Ma, Q.: CNMM: a grid-based spatially-distributed catchment simulation model, China Science Press, Beijing, 2017.

Liu, J., Ding, P., Zong, Z., Li, J., Tian, C., Chen, W., Chang, M., Salazar, G., Shen, C., Cheng, Z., Chen, Y., Wang, X., Szidat, S., Zhang, G.: Evidence of rural and suburban sources of urban haze formation in China: a case study from the Pearl River Delta region, J. Geophys. Res. - Atmos., 123, 4712–4726, doi:10.1029/2017jd027952, 2018.

Liu, T., Fan, D., Zhang, X., Chen, J., Li, C., Cao, C.: Deep placement of nitrogen fertilizers reduces ammonia volatilization and increases nitrogen utilization efficiency in no-tillage paddy fields in central China, Field Crops Res., 184, 80–90, doi:10.1016/j.fcr.2015.09.011, 2015.

Liu, X., Ju, X., Zhang, F., Pan, J., Christie, P.: Nitrogen dynamics and budgets in a winter wheat–maize cropping system in the North China Plain, Field Crops Res., 83, 111–124, doi:10.1016/S0378-4290(03)00068-6, 2003.

Mariano, E., de Sant Ana Filho, C. R., Bortoletto-Santos, R., Bendassolli, J. A., Trivelin, P. C. O.: Ammonia losses following surface application of enhanced-efficiency nitrogen fertilizers and urea, Atmos. Environ., 203, 242–251, doi:10.1016/j.atmosenv.2019.02.003, 2019.

Martens, D. A., Bremner, J. M.: Soil properties affecting volatilization of ammonia from soils treated with urea, Commun. Soil Sci. Plan., 20, 1645–1657, doi:10.1080/00103628909368173, 1989.

Martin, S. T., Hung, H. M., Park, R. J., Jacob, D. J., Spurr, R. J. D., Chance, K. V., Chin, M.: Effects of the physical state of tropospheric ammonium-sulfate-nitrate particles on global aerosol direct radiative forcing, Atmos. Chem. Phys., 4, 183–214, doi:10.5194/acp-4-183-2004, 2004.

Michalczyk, A., Kersebaum, K.C., Heimann, L., Roelcke, M., Sun, Q. P., Chen, X. P., Zhang, F. S.: Simulating in situ ammonia volatilization losses in the North China Plain using a dynamic soil-crop model, J. Plant Nutr. Soil Sc., 179, 270–285, doi:10.1002/jpln.201400673, 2016.

Mikkelsen, D. S., Datta, S. K. D., Obcemea, W. N.: Ammonia volatilization losses from flooded rice soils, Soil Sci. Soc. Am. J., 42, 725–730, doi:10.2136/sssaj1978.03615995004200050043x, 1978.

Park, K. D., Lee, D. W., Li, Y., Chen, D., Park, C. Y., Lee, Y. H., Lee, C. H., Kang, U. G., Park, S. T., Cho, Y. S.: Simulating ammonia volatilization from applications of different urea applied in rice field by WNMM, Korean J. Crop Sci., 53, 8–14, 2008.

Paulot, F., Jacob, D. J., Pinder, R. W., Bash, J. O., Travis, K., Henze, D. K.: Ammonia emissions in the United States, European Union, and China derived by high-resolution inversion of ammonium wet deposition data: Interpretation with a new agricultural emissions inventory (MASAGE_$NH_3$), J. Geophys. Res. - Atmos., 119, 4343–4364, doi:10.1002/2013jd021130, 2014.

Riddick, S., Ward, D., Hess, P., Mahowald, N., Massad, R., Holland, E.: Estimate of changes in agricultural terrestrial nitrogen pathways and ammonia emissions from 1850 to present in the Community Earth System Model, Biogeosciences, 13, 3397–3426, doi:10.5194/bg-13-3397-2016, 2016.

Roelcke, M., Li, S., Tian, X., Gao, Y., Richter, J.: In situ comparisons of ammonia volatilization from N fertilizers in Chinese loess soils, Nutr. Cycl. Agroecosys., 62, 73–88, doi:10.1023/a:1015186605419, 2002.

Sanz-Cobena, A., Misselbrook, T., Camp, V., Vallejo, A.: Effect of water addition and the urease inhibitor NBPT on the abatement of ammonia emission from surface applied urea, Atmos. Environ., 45, 1517–1524, doi:10.1016/j.atmosenv.2010.12.051, 2011.

Savard, M. M., Cole, A., Smirnoff, A., Vet, R.: $\delta^{15}$N values of atmospheric N species simultaneously collected using sector - based samplers distant from sources isotopic inheritance and fractionation, Atmos. Environ., 162, 11–22, doi:10.1016/j.atmosenv.2017.05.010, 2017.

Schjørring, J. K.: Atmospheric ammonia and impacts of nitrogen deposition: Uncertainties and challenges, New Phytol., 139, 59–60, doi:10.1046/j.1469-8137.1998.00173.x, 1998.

Sommer, S. G., Schjoerring, J. K., Denmead, O. T.: Ammonia emission from mineral fertilizers and fertilized crops, In: Sparks, D.L. editor, Advances in Agronomy, 82, 557–622, 2004.

Song, Y., Fan, X., Lin, D., Yang, L., Zhou, J.: Ammonia volatilization from paddy fields in the Taihu lake region and its influencing factors, Acta Pedologica Sinica, 265–269, doi:10.11766/trxb200306090216, 2004.

Tian, G., Cai, Z., Cao, J., Li, X.: Factors affecting ammonia volatilization from a rice–wheat rotation system, Chemosphere, 42, 123–129, doi: 10.1016/S0045-6535(00)00117-X, 2001.

Vira, J., Hess, P., Melkonian, J., and Wieder, W. R.: An improved mechanistic model for ammonia volatilization in Earth system models: Flow of Agricultural Nitrogen version 2 (FANv2), Geosci. Model Dev., 13, 4459–4490, doi: 10.5194/gmd-13-4459-2020, 2020.

Wang, H., Hu, Z., Lu, J., Liu, X., Wen, G., Blaylock, A.: Estimation of ammonia volatilization from a paddy field after application of controlled-release urea based on the modified Jayaweera-Mikkelsen model combined with the Sherlock-Goh model, Commun. Soil Sci. Plan., 47, 1630–1643, doi:10.1080/00103624.2016.1206120, 2016.

Xu, R., Tian, H., Pan, S., Prior, S. A., Feng, Y., Batchelor, W. D., Chen, J., Yang, J.: Global ammonia emissions from synthetic nitrogen fertilizer applications in agricultural systems: Empirical and process-based estimates and uncertainty, Global Change Biol., 25, 314–326, doi:10.1111/gcb.14499, 2019.

Zhan, X., Chen, C., Wang, Q., Zhou, F., Hayashi, K., Ju, X., Lam, S. K., Wang, Y., Wu, Y., Fu, J., Zhang, L., Gao, S., Hou, X., Bo, Y., Zhang, D., Liu, K., Wu, Q., Su, R., Zhu, J., Yang, C., Dai, C., Liu, H.: Improved Jayaweera-Mikkelsen model to quantify ammonia volatilization from rice paddy fields in China, Environ. Sci. Pollut. R., 26, 8136-8147, doi:10.1007/s11356-019-04275-2, 2019.

Zhang, S., Cai, G., Wang, X., Xu, Y., Zhu, Z., Freney, J. R.: Losses of urea-nitrogen applied to maize grown on a calcareous Fluvo-Aquic soil in North China Plain, Pedosphere, 171–178, doi:10.1109/34.142909, 1992.

Zhang, W., Li, S., Han, S., Xie, H., Lu, C., Sui, Y., Rui, W., Liu, C., Yao, Z., Zheng, X.: Less intensive nitrate leaching from Phaeozems cultivated with maize generally occurs in northeastern China, Agr. Ecosyst. Environ., doi:10.1016/j.agee.2021.107303, 2021.

Zhang, W., Li, Y., Zhu, B., Zheng, X., Liu, C., Tang, J., Su, F., Zhang, C., Ju, X., Deng, J.: A process-oriented hydro-biogeochemical model enabling simulation of gaseous carbon and nitrogen emissions and hydrologic nitrogen losses from a subtropical catchment, Sci. Total Environ., 616, 305–317, doi:10.1016/j.scitotenv.2017.09.261, 2018.

Zhang, W., Yao, Z., Zheng, X., Liu, C., Rui, W., Wang, K., Li, S., Han, S., Zuo, Q., Shi, J.: Effects of fertilization and stand age on $N_2O$ and NO emissions from tea plantations: a site-scale study in a subtropical region using a modified biogeochemical model, Atmos. Chem. Phys., 20, 6903–6919, doi:10.5194/acp-20-6903-2020, 2020.

Zhao, X., Xie, Y., Xiong, Z., Yan, X., Xing, G., Zhu, Z.: Nitrogen fate and environmental consequence in paddy soil under rice-wheat rotation in the taihu lake region, China, Plant Soil, 319, 225–234, doi: 10.1007/s11104-008-9865-0, 2009.

Zhou, F., Ciais, P., Hayashi, K., Galloway, J., Kim, D. G., Yang, C., Li, S., Liu, B., Shang, Z., Gao, S.: Re-estimating $NH_3$ emissions from Chinese cropland by a new nonlinear model, Environ. Sci. Technol., 50, 564–572, doi:10.1021/acs.est.5b03156, 2016.

Zhu, Z., Cai, G., Simpson, J. R., Zhang, S., Chen, D., Jackson, A. V., Freney, J. R.: Processes of nitrogen loss from fertilizers applied to flooded rice fields on a calcareous soil in north–central China, Nutr. Cycl. Agroecosys., 18, 101–115, doi:10.1007/BF01049507, 1989.

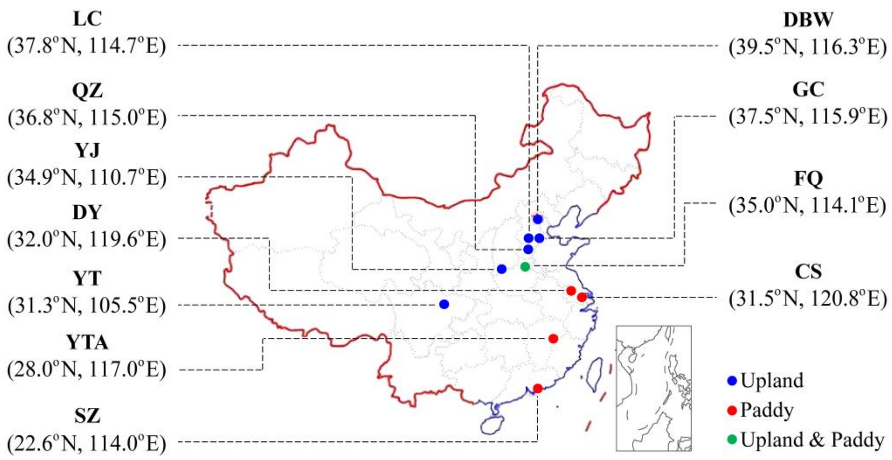


**Fig. 1 Location of the experimental field sites involved in this study. The sites are Changshu (CS), Danyang (DY), Dongbeiwang (DBW), Fengqiu (FQ), Guangchuan (GC), Luancheng (LC), Quzhou (QZ), Shenzhen (SZ), Yanting (YT), Yingtan (YTA), and Yongji (YJ).**

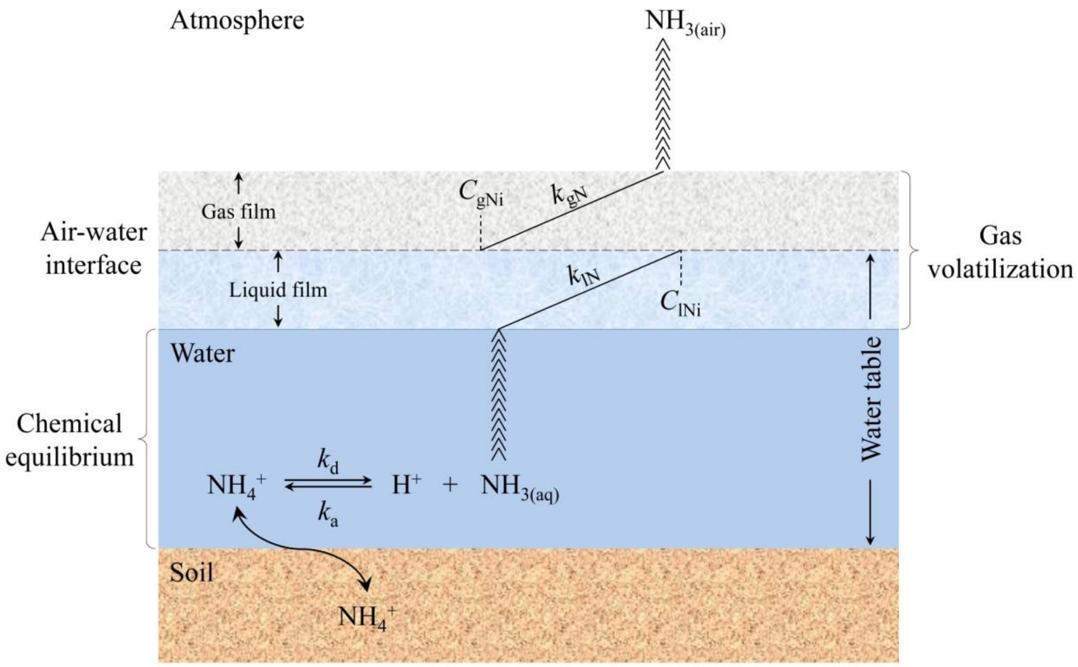


**Fig. 2 Mechanism of the Jayaweera-Mikkelsen model introduced into the modified CNMM-DNDC. $k_d$ and $k_a$ are referred to as the dissociation and association rate constants for $NH_4^+/NH_3$ chemical equilibrium, respectively. $k_{lN}$ and $k_{gN}$ are referred to as the exchange constants for $NH_3$ in the liquid and gas films, respectively. $C_{lNi}$ and $C_{gNi}$ are referred to as the average concentrations of $NH_3$ at the interface in the liquid and gas films, respectively. $NH_{3(aq)}$ and $NH_{3(air)}$ are referred to as the average concentration of $NH_3$ in aqueous and gas phases, respectively.**

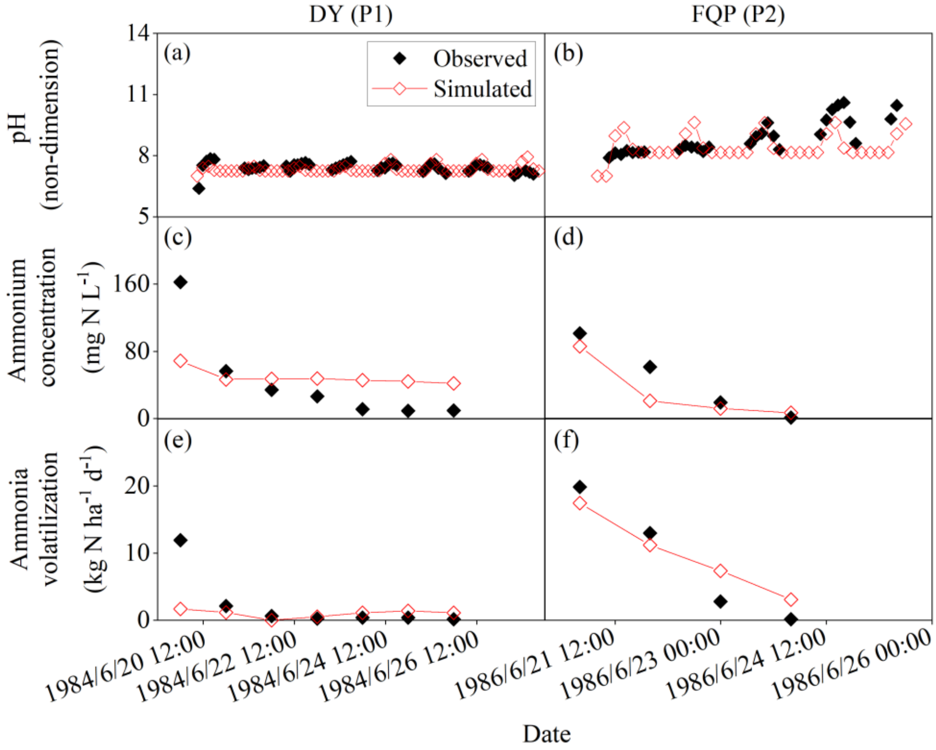


**Fig. 3 Observed and simulated pH and ammonium concentrations of floodwater and daily ammonia volatilization from the ammonium carbonate application for DY and FQP. The definitions of the case codes are referred to Table 2. The sites are Danyang (DY) and Fengqiu with rice paddy fields (FQP).**

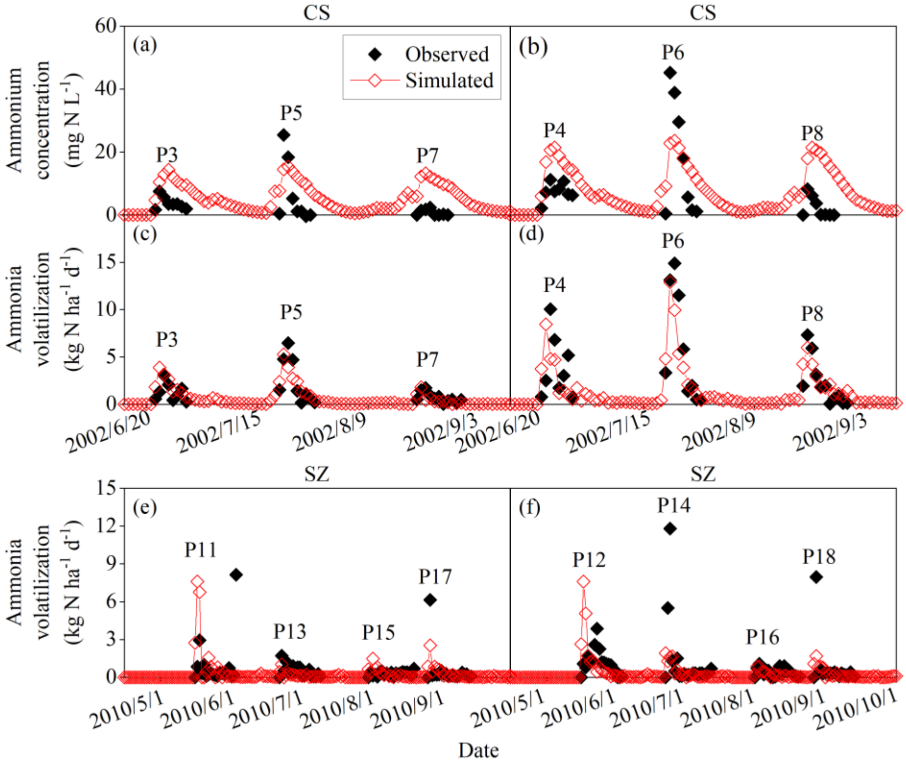


**Fig. 4 Observed and simulated ammonium concentrations of floodwater and daily ammonia volatilization from the urea application for CS and SZ. The definitions of the case codes are referred to Table 2. The sites are Changshu (CS) and Shenzhen (SZ).**

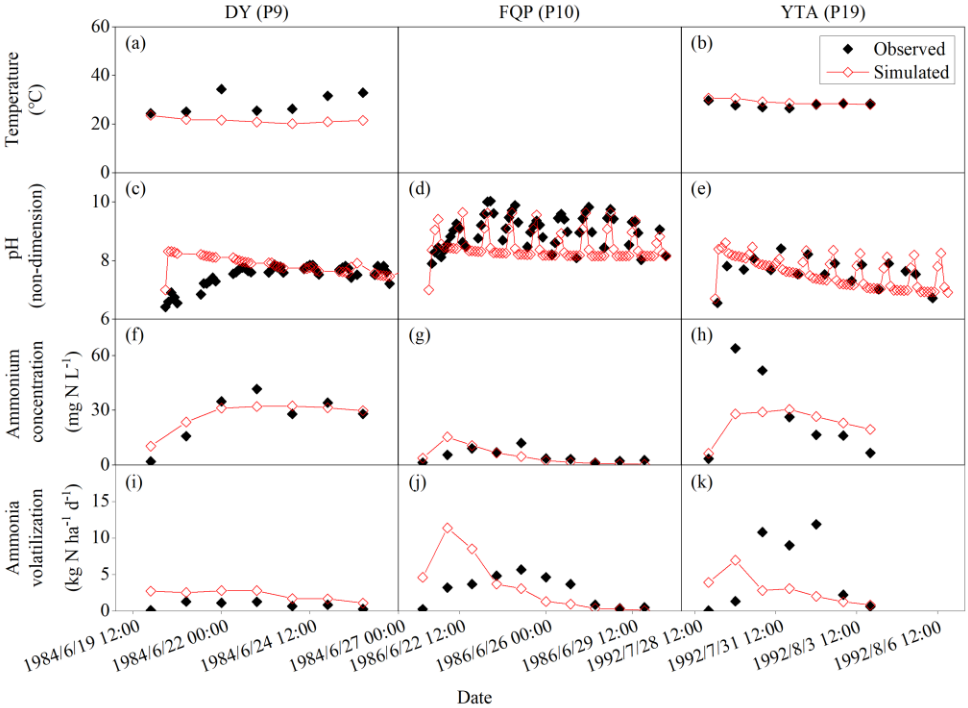


**Fig. 5 Observed and simulated temperatures, pH and ammonium concentrations of floodwater and daily ammonia volatilization from the urea application for DY, FQP and YTA. The definitions of the case codes are referred to Table 2. The sites are Danyang (DY), Fengqiu with rice paddy fields (FQP) and Yingtan (YTA).**

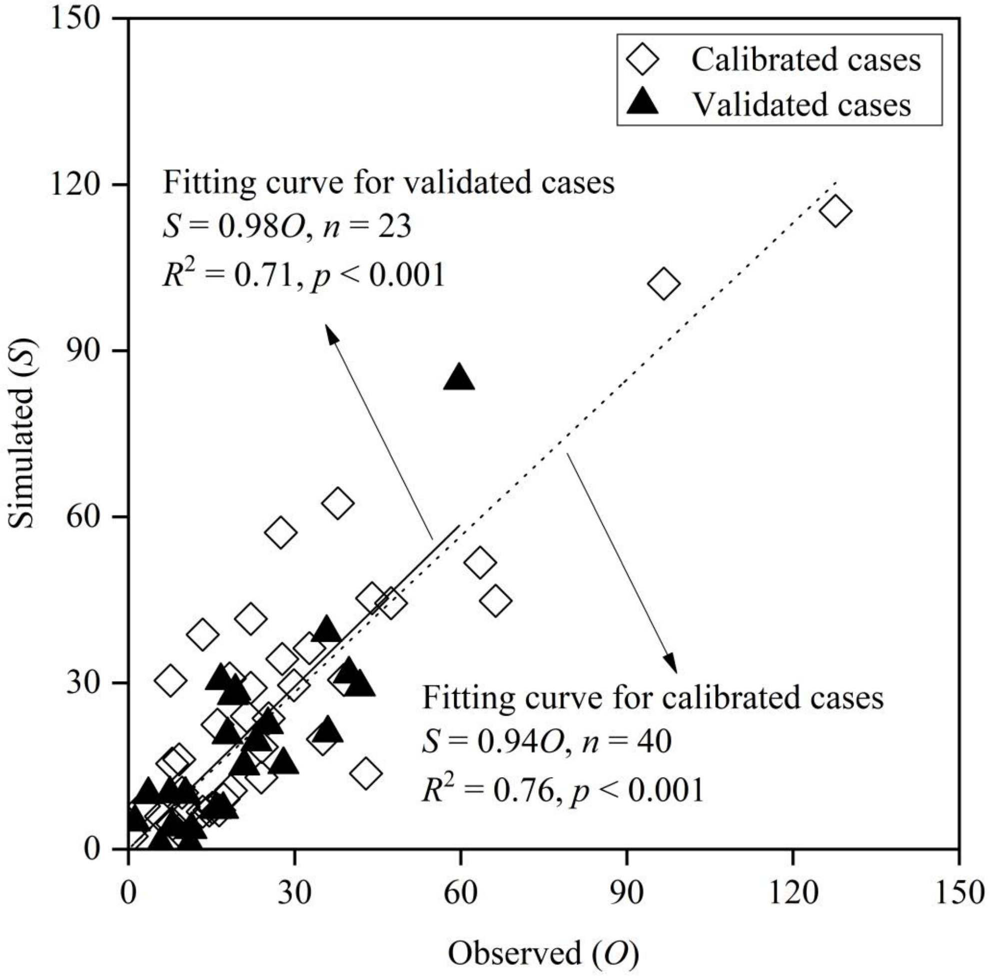


**Fig. 6 Comparison between the observed and simulated cumulative ammonia volatilization across all calibrated and validated cases of upland and rice paddy fields. *n, p* and $R^2$ denote the sample size, significance level and coefficient of determination for the zero-intercept linear regression, respectively.**

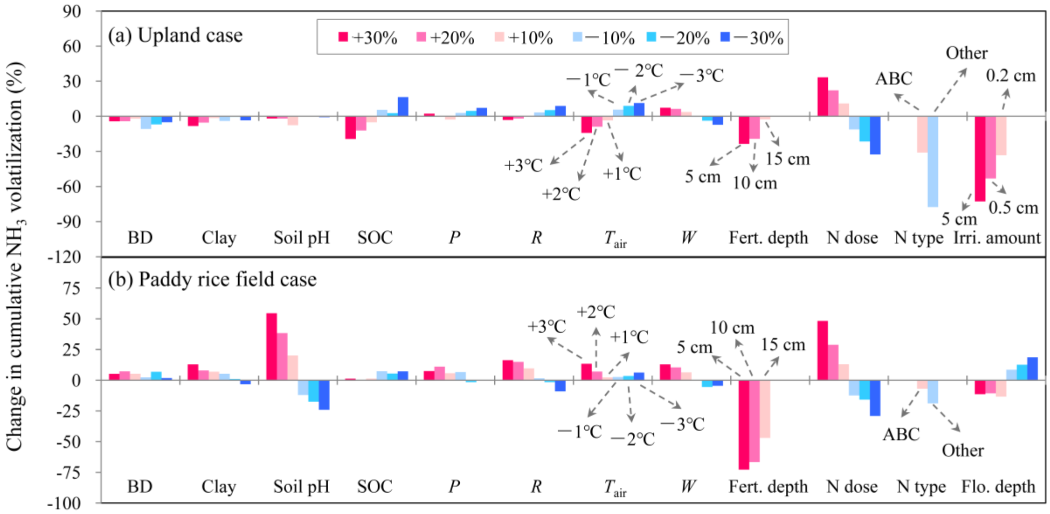


**Fig. 7 Sensitivity analysis of the modified CNMM-DNDC in simulating cumulative ammonia ($NH_3$) volatilization from uplands and rice paddy fields during the measurement periods through change input factors. The investigated input factors include: 3-hourly averages of air temperature ($T_{air}$) and wind speed (*W*); 3-hourly totals of precipitation (*P*) and solar radiation (*R*) during individual measurement periods of $NH_3$ volatilization; soil clay fraction, pH, organic carbon (SOC) content and bulk density (BD); irrigation water amount (Irri. amount) and floodwater depth (Flo. depth); and, nitrogen fertilization depth, dose and type (Fert. depth, N dose, and N type, respectively). The N types include ammonium bicarbonate (ABC) and other ammonium-based nitrogen fertilizers (Other). The legends within the frame apply to all the subfigures and all the factors without notes highlighted by arrows.**

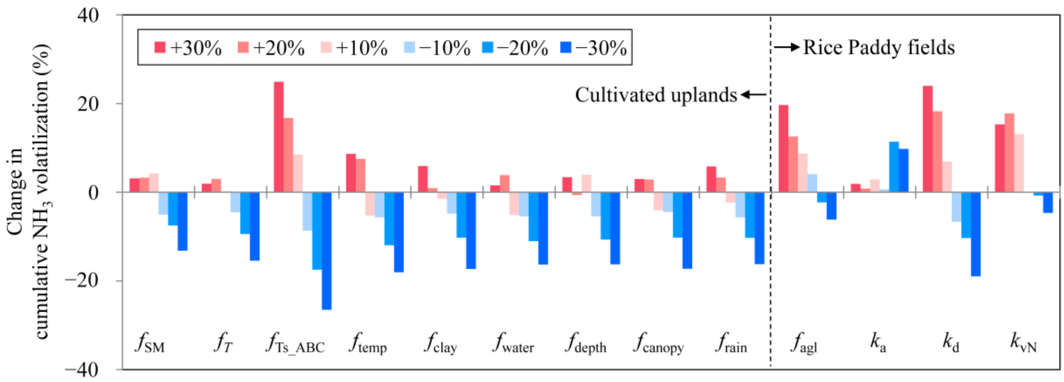


**Fig. 8 Sensitivity analysis on the improved parameters of the modified CNMM-DNDC model in simulating cumulative ammonia ($NH_3$) volatilization from cultivated uplands and rice paddy fields. The improved parameters for simulating $NH_3$ volatilization from cultivated uplands involved in the sensitivity analysis include: effect of soil moisture and soil temperature on urea hydrolysis ($f_{SM}$ and $f_T$), effect of soil temperature on ammonium bicarbonate decomposition ($f_{Ts\_ABC}$), effect of soil temperature, soil clay content, soil moisture, soil depth, dry canopy, rain wetting canopy on $NH_3$ volatilization ($f_{temp}$, $f_{clay}$, $f_{water}$, $f_{depth}$, $f_{canopy}$ and $f_{rain}$). The improved parameters for simulating $NH_3$ volatilization from rice paddy fields involved in the sensitivity analysis include: the effect of algal growth on floodwater pH ($f_{alg}$), the dissociation and association rate constants for $NH_4^+/NH_{3(aq)}$ equilibrium ($k_d$ and $k_a$), and the volatilization rate constant of $NH_{3(aq)}$ ($k_{vN}$).**

**Table 1** Descriptive information of the studied experimental sites of rice paddy fields for model evaluation, including site name, experimental year (Year), crop rotation (Crop), fertilizer type (Type) and dose (Dose, kg N $ha^{-1}$), measurement method for ammonia volatilization (Method), number of fertilization cases (Number) and reference (Ref.).

| Site [a] | Year | Crop [b] | Type | Dose | Method [d] | Number | Ref. [e] |
|---|---|---|---|---|---|---|---|
| CS | 2002–2003 | RW | Urea | 41–135 | MM | 6 | [1] |
| DY | 1984 | RW | Urea/ABC [c] | 90 | MM | 2 | [2] |
| FQP | 1986 | RW | Urea/ABC | 90 | MM | 2 | [3] |
| SZ | 2010 | DR | Urea | 41–162 | WT | 8 | [4] |
| YTA | 1992 | DR | Urea | 90 | MM | 1 | [5] |

[a] The sites are Changshu (CS), Danyang (DY), Fengqiu with rice paddy fields (FQP), Shenzhen (SZ), and Yingtan (YTA).

[b] The presented crop rotation types are rice–wheat (RW) and double rice (DR).

[c] ABC is the abbreviation of ammonium bicarbonate.

[d] The presented methods for the measurement of ammonia volatilization are wind tunnel (WT) and micrometeorological technique (MM).

[e] [1] Song et al., 2004; [2] Cai et al., 1986; [3] Zhu et al., 1989; [4] Gong et al., 2013; and [5] Cai et al., 1992.

**Table 2** Observed and simulated cumulative ammonia volatilization during the measurement periods, model biases, and management practices of individual fertilizer application cases in the rice paddy fields.

| Case code [a] | Site [b] | Period | *O* [c] | *S* [c] | RMB [c] | Water table [d] | Pre[e] | Fertilizer application | | |
|---|---|---|---|---|---|---|---|---|---|---|
| | | | | | | | | Type [f] | Method [g] | Dose [h] |
| P1[@] | DY | Jun. 20 to Jun. 26, 1984 | 16.4 | 7.04 | −57.0 | 5 | 0 | ABC | BFT5 | 90 |
| P2 | FQP | Jun. 21 to Jun. 30, 1986 | 35.8 | 39.13 | 9.3 | 4 | 0.18 | ABC | BFT5 | 90 |
| P3 | CS | Jun. 22 to Jun. 30, 2002 | 10.3 | 9.89 | −4.0 | 4[*] | 6.38 | Urea | B | 40.5 |
| P4 | CS | Jun. 22 to Jun. 30, 2002 | 23.1 | 19.40 | −16.0 | 4[*] | 6.38 | Urea | B | 81 |
| P5 | CS | Jul. 20 to Jul. 29, 2002 | 20.9 | 15.04 | −28.0 | 4[*] | 0.54 | Urea | B | 54 |
| P6 | CS | Jul. 20 to Jul. 29, 2002 | 39.8 | 31.61 | −20.6 | 4[*] | 0.54 | Urea | B | 108 |
| P7 | CS | Aug. 20 to Aug. 31, 2002 | 7.5 | 10.02 | 33.6 | 4[*] | 3.07 | Urea | B | 40.5 |
| P8 | CS | Aug. 20 to Aug. 31, 2002 | 17.9 | 20.68 | 15.5 | 4[*] | 3.07 | Urea | B | 81 |
| P9[@] | DY | Jun. 20 to Jun. 26, 1984 | 7.9 | 15.44 | 94.9 | 5 | 0 | Urea | BFT5 | 90 |
| P10[@] | FQP | Jun. 21 to Jun. 30, 1986 | 27.8 | 34.32 | 23.7 | 4 | 0.18 | Urea | BFT5 | 90 |
| P11[@] | SZ | May 16 to Jun. 4, 2010 | 16.1 | 22.50 | 39.8 | 7.5[#] | 0 | Urea | B | 162.2 |
| P12[@] | SZ | May 16 to Jun. 4, 2010 | 21.4 | 24.00 | 12.2 | 7.5[#] | 0 | Urea | B | 162.2 |
| P13[@] | SZ | Jun. 22 to Jul. 11, 2010 | 9.1 | 3.43 | −62.4 | 7.5[#] | 0 | Urea | B | 40.9 |
| P14[@] | SZ | Jun. 22 to Jul. 11, 2010 | 17.2 | 9.07 | −47.3 | 7.5[#] | 0 | Urea | B | 81.8 |
| P15[@] | SZ | Jul. 31 to Aug. 19, 2010 | 5.9 | 5.92 | 0.3 | 7.5[#] | 0 | Urea | B | 40.9 |
| P16[@] | SZ | Jul. 31 to Aug. 19, 2010 | 8.0 | 4.57 | −42.9 | 7.5[#] | 0 | Urea | B | 40.9 |
| P17[@] | SZ | Aug. 26 to Sep. 14, 2010 | 10.0 | 7.66 | −23.4 | 7.5[#] | 0 | Urea | B | 81.8 |
| P18[@] | SZ | Aug. 26 to Sep. 14, 2010 | 13.4 | 6.79 | −49.3 | 7.5[#] | 0 | Urea | B | 81.8 |
| P19 | YTA | Jul. 29 to Aug. 6, 1992 | 36.0 | 20.98 | −41.7 | 2 | 1.36 | Urea | BFT5 | 90 |

[a] P1 to P19 encode the experimental cases following individual application events of synthetic nitrogen fertilizers; the superscript "@" symbol marks the cases with the ammonia observations being referred to the model calibration.

[b] The sites are Changshu (CS), Danyang (DY), Fengqiu with rice paddy fields (FQP), Shenzhen (SZ), and Yingtan (YTA).

[c] *O* and *S* are the cumulative $NH_3$ volatilization (kg N $ha^{-1}$) observed and simulated by the modified CNMM-DNDC, respectively; RMB is the relative model bias (%) of the modified model, each of which was determined as the relative difference between the simulated and observed values.

[d] The depth of floodwater table (cm). For the cases with "*" and "#", the exact depth of the floodwater table was not reported. The floodwater table depth of the cases with "*" was arbitrarily set as the traditional depth of the floodwater table of the DY site, which was located in the same region. The floodwater depths of the cases with "#" were set by model calibration.

[e] Pre denotes total rainfall (cm) during the experimental period(s).

[f] ABC is the fertilizer type of ammonium bicarbonate.

[g] The application methods are surface broadcast (B) and broadcast followed by tillage (BFT). The figures following BFT are the depth in soil (cm).

[h] Unit: kg N $ha^{-1}$.

**Table 3** Statistical indices for evaluating the performance of the modified CNMM-DNDC in simulating daily and cumulative ammonia ($NH_3$) fluxes from ammonium bicarbonate (ABC) and urea (including other fertilizer types) applications for the independent calibration (Cal) and validation (Val) cases in uplands and rice paddy fields.

| Land use | $NH_3$ flux | Fertilizer type | Operation | Num | IA | NSI | ZIR | | |
|---|---|---|---|---|---|---|---|---|---|
| | | | | | | | Slope | $R^2$ | $p$ |
| Upland | Daily | ABC | Cal | 39 | 0.5 | –1.34 | 0.53 | na | na |
| | | | Val | 24 | 0.60 | –0.51 | 0.69 | na | na |
| | | Urea | Cal | 287 | 0.44 | –0.06 | 0.38 | na | na |
| | | | Val | 137 | 0.67 | 0.02 | 0.64 | 0.09 | < 0.001 |
| | Cumulative | ABC | Cal | 3 | 0.75 | 0.14 | 0.73 | 0.64 | ns |
| | | | Val | 2 | – | – | – | – | – |
| | | Urea | Cal | 26 | 0.93 | 0.73 | 0.94 | 0.71 | < 0.001 |
| | | | Val | 13 | 0.91 | 0.49 | 1.06 | 0.74 | < 0.001 |
| Rice paddy field | Daily | ABC | Cal | 7 | 0.33 | 0.02 | 0.16 | na | na |
| | | | Val | 4 | 0.94 | 0.85 | 0.90 | 0.71 | ns |
| | | Urea | Cal | 176 | 0.53 | –0.35 | 0.47 | 0.04 | < 0.05 |
| | | | Val | 63 | 0.72 | 0.36 | 0.56 | 0.19 | < 0.001 |
| | Cumulative | ABC | Cal | 1 | – | – | – | – | – |
| | | | Val | 1 | – | – | – | – | – |
| | | Urea | Cal | 10 | 0.88 | 0.30 | 1.03 | 0.68 | < 0.01 |
| | | | Val | 7 | 0.85 | 0.60 | 0.77 | 0.65 | < 0.05 |

The statistical indices are the index of agreement (IA), Nash–Sutcliffe Index (NSI), and the slope, determination coefficient ($R^2$) and significance level ($p$) of the zero-intercept univariate linear regression (ZIR) of observations against simulations. Being not available (na) indicates a negative $R^2$ and a suffering $F$-test. Being not significant (ns) indicates a ZIR with $p > 0.05$. Num is the abbreviation of sample number.

**Table 4** Statistical indices for evaluating the performance of the CNMM-DNDC in simulating the daily temperature (*T*), pH and ammonium concentration ($NH_4^+$) in floodwater for the calibration (Cal) and validation (Val) cases.

| Variables | Operation | Num | Cases | IA | NSI | ZIR | | |
|---|---|---|---|---|---|---|---|---|
| | | | | | | Slope | $R^2$ | *p* |
| *T* | Cal | 7 | P9 | 0.43 | –3.50 | 1.32 | na | na |
| | Val | 7 | P19 | 0.51 | –1.76 | 0.96 | na | na |
| pH | Cal | 147 | P1, P9, P10 | 0.83 | 0.55 | 1.00 | 0.55 | < 0.001 |
| | Val | 45 | P2, P19 | 0.79 | 0.36 | 1.01 | 0.36 | < 0.001 |
| $NH_4^+$ | Cal | 24 | P1, P9, P10 | 0.78 | 0.48 | 1.03 | 0.48 | < 0.001 |
| | Val | 55 | P2, P3–P8 | 0.68 | 0.25 | 0.74 | 0.34 | < 0.001 |

The statistical indices are the index of agreement (IA), Nash–Sutcliffe Index (NSI), and the slope, determination coefficient ($R^2$) and significance level (*p*) of the zero-intercept univariate linear regression (ZIR) of observations against simulations. Being not available (na) indicates a negative $R^2$ and a suffering *F*-test. Being not significant (ns) indicates a ZIR with $p > 0.05$. Num is the abbreviation of sample number. The definitions of the case codes are referred to Table 2.